ZIBELINE INTERNATIONAL™ PUBLISHING

ISSN: 2521-0920 (Print)
ISSN: 2521-0602 (Online)
CODEN: MJGAAN

Malaysian Journal of Geosciences (MJG)

DOI: http://doi.org/10.26480/mjg.02.2023.96.105

CrossMark

RESEARCH ARTICLE

AQUIFER SYSTEMS CHARACTERIZATION FOR GROUNDWATER MANAGEMENT IN ILE-OLUJI, SOUTHWESTERN NIGERIA, USING MCDA GIS-BASED AHP

O.O. Falowo*, Y. Akindureni, O.C. Babalola

Federal University of Technology Akure, Ondo State, Nigeria
Department of Civil Engineering Technology, Rufus Giwa Polytechnic, Owo, Ondo State, Nigeria
**Corresponding Author Email: oluwanifemi.adeboye@yahoo.com*

ARTICLE DETAILS

Article History:

Received 23 May 2023
Revised 01 June 2023
Accepted 14 July 2023
Available online 17 July 2023

ABSTRACT

Multicriteria decision analysis for groundwater potential mapping utilizing analytical hierarchical process of six hydrogeologic parameters including aquifer layer thickness, aquifer layer resistivity, overburden thickness, transverse resistance, transmissivity, and coefficient of anisotropy; in relation to groundwater yield was carried out in Ile Oluji, Southwestern Nigeria. The aim was to develop groundwater potential map using calculated groundwater potential index values (GWPIV). The obtained GWPIV which ranged from 1.53 (granite) – 3.50 (migmatite) with an average of 2.18 suggestive of moderate groundwater potential (90 % of the study area). The low potential zone (10 %) are observed sporadically in the central and northwestern parts. All the geological units recorded overlapping hydrogeologic properties. The longitudinal unit conductance recorded regional average of 0.219876 mhos. Therefore the protective capacity of groundwater system in the study area is weak, and relatively less-weaker in granite environment; and in northwestern and central parts. Nevertheless, the water table aquifer (accounts for 80%) and the fracture basement (constitutes 20%, frequently occurring in gneissic environment) are the water bearing units, with average overburden thickness in migmatite, granite, and gneiss 24.3 m, 24.5 m, and 27.9 m respectively. The average coefficient of anisotropy (1.12); hydraulic conductivity (0.37 m/d), transmissivity 6.86 m^2/d (migmatite: 7.17 m^2/d, granite: 7.14 m^2/d, and gneiss: 6.02 m^2/d). Hence gneissic offered both thick weathered layer and fractured aquifer. Empirical model for plot of formation factor and hydraulic conductivity in migmatite, granite, and gneiss, showed positive correlations in descending order as: granite (0.3778), migmatite (0.1057), and gneiss (0.0641).

KEYWORDS

Groundwater Yield, Aquifer Properties, Hydrogeologic, Geographic Information System, Borehole Section

1. INTRODUCTION

An aquifer is a geological entity capable of storing and delivering significant quantities of water for a variety of uses (Fetter, 2007). Groundwater is defined as underground fresh water that can be extracted for domestic, agricultural, and commercial uses. Many shallow and deep aquifers/groundwater bodies have been investigated, and significant levels of contaminants have been discovered. Thus, assessment of groundwater supply has become an important and critical task for current and future groundwater quality management (Falowo and Daramola, 2023; Cosgrove and Loucks, 2015; Bayewu et al., 2018; Sajeena et al., 2014). This is so, because of special characteristics of groundwater, as they are not easily degraded or exhausted like surface water, abundant aquifers are an important source of water supply in terms of quality and availability. They are generally available, reliable, and simple to use (Fetter, 2007). Groundwater quality is influenced by the quality of recovered water, atmospheric rainfall, freshwater surface water, and subsurface geochemical processes. Changes in the origin and makeup of recharged water, as well as hydrologic and human variables, can also result in occasional changes in ground water quality (Sameer et al., 2021; Gao et al., 2018; Falowo et al., 2017). A region's geology has a major influence on the mineral content of water and its environs. The chemical composition of the nearby sediments and subsoil alters the nature of groundwater. Modern civilization and growth, as well as the frequent release of industrial effluent, domestic sewage, and solid garbage dumps, all contribute to groundwater pollution. When groundwater becomes polluted, it poses a threat to human health, economic development and social prosperity (Falowo et al., 2017; Ting, 1993; Omer, 2018; Alley and Leake, 2004; Bayewu et al., 2018; (Falowo and Daramola, 2023; Cosgrove and Loucks, 2015; Sajeena et al., 2014).

Groundwater accounts for 98% of the world's fresh water, as a result, the sustainable provision of groundwater supplies for current and future needs is of regional to global significance (Mandel and Shiftan, 1981; Karanth, 1987). Groundwater research includes all activities that lead to the identification of aquifers or underground pools from which water can be obtained in adequate quantity and quality for the intended purpose (Harvill and Bell, 1986; Mohamaden, 2016). Groundwater resources are critical to the longevity and viability of human life on Earth, as they are used for drinking, municipal, domestic, industrial, and agricultural reasons (Lewis, 1989; Akinrinade and Olabode, 2015; Harb et al., 2010). It exists on earth and is irregularly distributed in time and space (Akinrinade and Adesina, 2016; Chaanda and Alaminiokuma, 2020). However, global development and population increase have put an excessive burden on the environment resulting in overexploitation and uncontrolled bore well sinking (Oyegoke et al., 2020). Groundwater sustainability and administration is becoming an important subject of debate at the United Nations Congress as a consequence of the Millennium Goals (Falowo and

Quick Response Code	Access this article online	
	Website: www.myjgeosc.com	DOI: 10.26480/mjg.02.2023.96.105

Cite The Article: O.O. Falowo, Y. Akindureni, O.C. Babalola (2023). Aquifer Systems Characterization for Groundwater Management in Ile-Oluji, Southwestern Nigeria, Using MCDA Gis-Based AHP. *Malaysian Journal of Geosciences, 7(2): 96-105.*

Daramola, 2023; Cosgrove and Loucks, 2015; Fetter, 2007; Adagunodo et al., 2018; Akanbi, 2016; Bayewu et al., 2018).

Geophysical studies, borehole recording, hydrogeological measurement, geologic mapping, and pumping tests are some of the most effective methods of evaluating an ecosystem without meddling with the hydrogeological system. However, the geophysical method involving the vertical electrical sounding (VES) method has been frequently used in groundwater exploration to identify the geoelectric parameters in terms of thickness and resistivity of the subsurface layers, as well as their hydrogeologic properties. Hence, geophysical method combining electrical resistivity has demonstrated to be efficient and cost-effective (Bayewu et al., 2018; Falowo, 2022; Adagunodo et al., 2018; Aina et al., 2019). Overburden thickness/depth to bedrock, fissure structure, and topography can all aid in identifying the ideal location for a borehole. Groundwater studies, mineral mining, engineering and environmental studies, investigative geology, and archaeological research all benefit from electrical's versatility (Robinson and Coruh, 1988; Telford et al., 1990). Because it identifies the vertical variation with depth of electrical resistance (resistivity) at a particular location, vertical electrical resistivity is the most frequently used technique for groundwater exploration. Passing an electric current (dc or ac) through current electrodes into the ground and detecting the potential difference between potential electrodes is the technique (Telford et al., 1990).

Borehole water failures and a lack of high-quality water have distressed the people of Ile Oluji in the last ten years as the population has increased tremendously (Tartiyus et al., 2015) The establishment of the Federal Polytechnic Institute in the area has attracted small and medium-sized businesses/industry, as well as increased individual property ownership. As a consequence, the region's existing groundwater supply infrastructure has been put under undue pressure, and it calls for productive exploration and exploitation of groundwater, which is one of the essential natural resource required for existence of life in the world. Aquifer thickness, as well as the extent and degree of interconnection of pore spaces within the aquifer substance, are known to influence the calculation of groundwater supplies (Freeze and Cherry, 1979; Bell, 2007). The region is part of the Basement Complex, which is distinguished by weathered and fractured rocks that are susceptible to surface or near-surface pollutants because they frequently appear at shallow levels. As a result, effective groundwater excavation in a basement topography necessitates a thorough knowledge of the hydrogeological features of the aquifer units in connection to their vulnerability to environmental pollution, as well as an evaluation of their protective capacity.

As a result, the sole aim of this study is to gain more understanding on the hydrogeological system in Ile Oluji, in order to define aquifers and target pollution-free groundwater to ensure the resource's long-term use. This research objectives included assessing the area's groundwater potential, determining the aquifer protective capacity of the overlying rocks, particularly its isolation from pollution, and suggesting appropriate groundwater placement locations. Furthermore, the findings of this research are anticipated to add to the creation of a practical control and mitigation strategy for the resource's future use in household, commercial, and farming applications. Furthermore, this will supplement the government's efforts in groundwater management strategies, especially the avoidance of groundwater quality degradation. The study employed direct (geological mapping, geomorphology, groundwater level measurement and pumping test) and indirect method using geoelectric method and its derived parameters to obtain the objectives of this study. The obtained data from both investigations were subjected to multi-criteria decision technique utilizing analytical hierarchy process (AHP). AHP is one of the most widely used multi-criteria choice techniques described in the literature and entails creating a number of pair-wise comparison grids that compare the criteria to one another (Saaty, 1980). The comparison is carried out to determine a rating or weight for each criterion; this rating describes the degree to which each criterion contributes to the general goal (Saaty, 2006). AHP is capable of recording both subjective and objective evaluation measures, as well as providing a helpful method for checking the coherence of the evaluation measures and options proposed by specialists or decision makers, thereby decreasing decision-making prejudice (Vargas, 1990).

1.1 Location and Geology of the Study Area

Ile Oluji is the study location, which is situated between 704800 m and 708800 m East and 793350 m and 809900 m North (Figure 1). It is bordered by Ipetu – Ijesa, Ondo East/West, Ifetedo, Okeigbo, and Ifedore local government areas. The area is characterized by Otasun Hills, Ikeji hills, Okurughu, Oni river and Awo rivers (Adebawore et al., 2017). It has a geographical area of 600 km^2 and a population of approximately 300,000 individuals. The landscapes of Ile-Oluji can be classified into three types: plains, undulating slopes, and river valleys. The mountains, on the other hand, dominate the landscape. The town is surrounded by many granite boulders, including Ota-Ororo, Ota-Akoko, Ota-Didu, Ota-Upote, and Iguruguru (Adebawore et al., 2017). The town serves as the headquarters of Ile-Oluji/Okeigbo Local Government. Ile Oluji is an agravian town, it is one of the largest producers and exporters of Cocoa production in Nigeria. Cassava, yam, maize and oil palm are the major crops cultivated by farmers in the town. The major manufacturing company in the town is Cocoa Products Ile Oluji Limited. The Federal Polytechnic, Ile Oluji is a major tertiary institution in the town while Gboluji Grammar school is the major high school in the area, and this school happens to be one of the oldest secondary school in Nigeria. The area is within the tropical rain forest with distinct wet and dry seasons. The annual rainfall varies between 1400 mm and 1800 mm. The mean temperature is 27°C and varies from 24.5°C in July to 29.5°C in February (Iloeje, 1981)

1.2 Geology

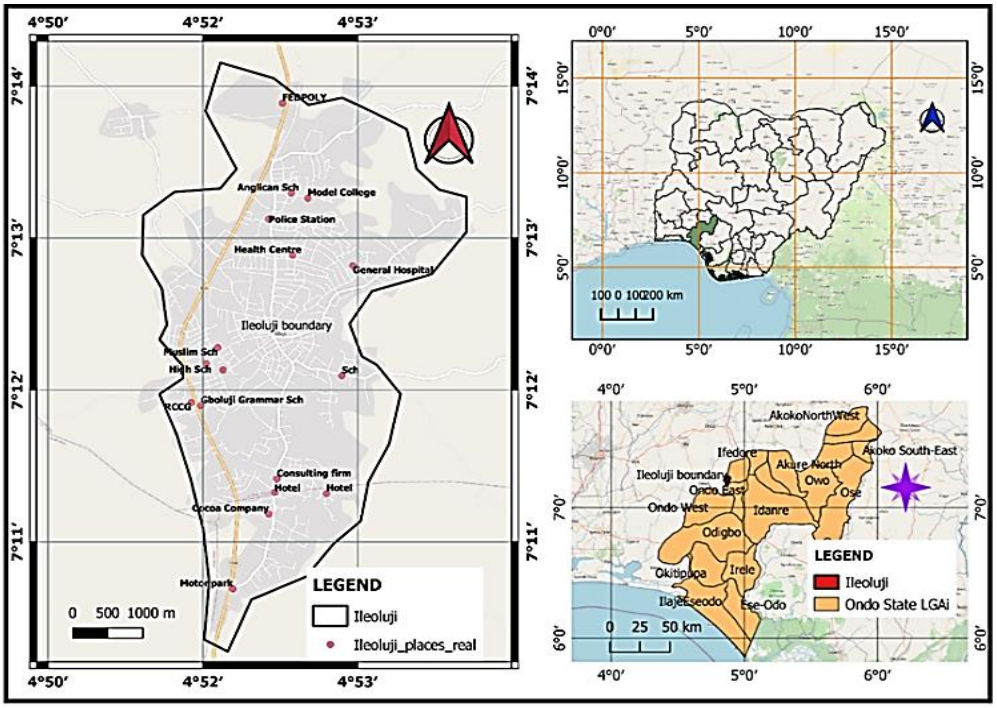

Figure 1: Location map of the Study Area on map of Ondo State and Nigeria

The study area is underlain by impermeable Precambrian basement materials. (Figure 2). Granites, quartzite, and migmatite-gneiss were among the local geological rock types identified from specimens. Quartzite (ridges) and granite gneiss are the most common, with granite gneiss occurring as intruding, low-lying formations. Field examination reveals the presence of joints, fractures, or fissures within the bedrock. As a result, there is a greater likelihood of these characteristics at greater depth, as this is one of the basement complex's peculiarities (i.e. fault, incipient joints, and fracture systems) that are a result of continuous tectonic/orogenic processes. In a typical basement environments, the fractured zone and weathered layer are the main aquiferous components. Often, difficulty are experienced in deciphering prolific aquifer in the basement and define its geometry, hence accurate knowledge of hydrogeological properties of the aquifer units and its susceptibility to environmental contamination is very important. The rocks mapped in the study area are granite, gneiss, migmatite (Figure 3).

The granitic rocks are rich in quartz, feldspar, and accessory mica (muscovite, biotite), amphiboles (hornblende), augite, hyperstene, magnetic, apatite, garnet, and tourmaline (Obaje, 2009). Their texture ranged from medium to coarse grained, while some are porphyritic (Figure 3a). The gneisses are megascopically crystalline foliated metamorphic rocks. They are characterized with mineral segregation into layers or bands of contrasting colour, texture and composition. Its common minerals are mica, feldspar, hornblende and quartz. The texture is medium to coarse with poor mineral arrangement. The gneisses show bands of micaceous minerals alternating with bands of equidimensional minerals like feldspar, quartz (Figure 3b). The migmatite are mixed rocks that consist of intimately associated members of igneous rock (granitic rock) and metamorphic (gneisses) groups, they are widespread in the study area.

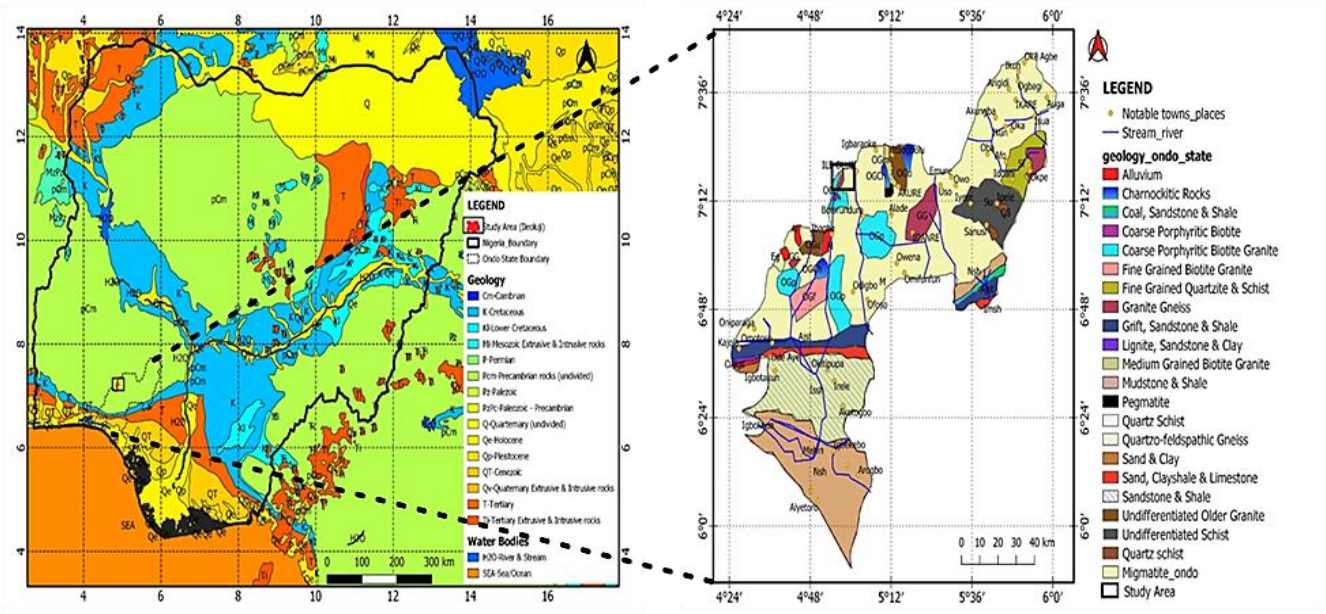

Figure 2: Geological map of (a) Nigeria and (b) Ondo State showing the study area, which falls within the Southwestern Basement Complex Nigeria with migmatite being the predominant rock unit. (0Modified after NGSA, 2006)

(a) Surface exposures and outcrops of granite at different locations having being subjected to intense weathering, some occuring as boulders with noticeable fractures/fissures. In addition feldspathic and quartzo-feldspathic intrusion are observed

(b) Surface exposures and outcrops of migmatites and granite gneiss at different locations having being subjected to intense weathering, with noticeable fractures/fissures. In addition feldspathic and quartzo-feldspathic intrusion are also observed

Figure 3: Surface exposure/outcrops of (a) granite (b) gneiss, and migmatite observed in the study area

1.3 Landuse and Soil

The landuse/land cover of the study area in Figure 4a is primarily built-up, with tree plantation and agricultural practices common in the town's outskirts, though few plantations are observed within the town; and the soil type in the area is ferric luvisols. (Figure 4b). The luvisols are soils with pronounced textural difference within the soil profile, with the top horizon drained of clay and clay buildup in a subsurface "Argic" horizon. Luvisols have high activity clays throughout and no sudden textural shift, whereas ferric luvisols have ferric characteristics.

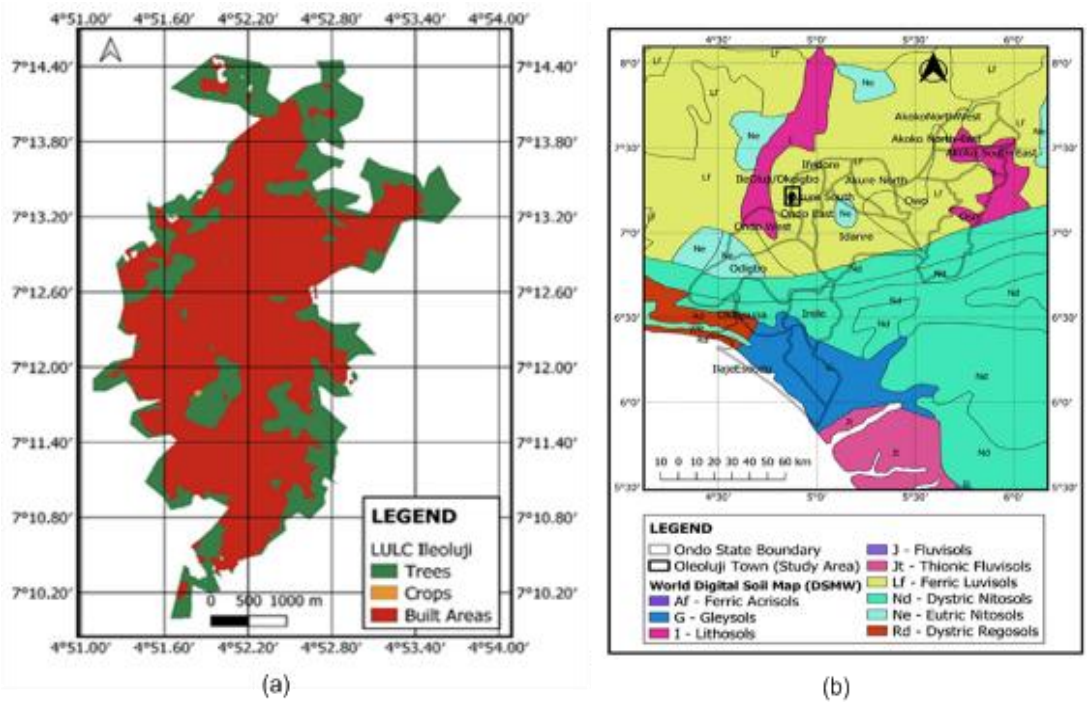

Figure 4: (a) The land use/land cover of the study area which is predominantly built up area (b) Soil map of Southwestern Nigeria, with the study area falling on Ferric Luvisols. Modified after Living Atlas, 2020; and FAO/DSMW, 2020 respectively)

The terrain analysis involving digital elevation model (DEM), hill shade, slope, and aspect (direction of slope) was produced using Quantum Geographic information system (QGIS) software. The elevation raster data/shape file was acquired from USGS website (earthexplorer-USGS) using SRTM 1 Arc Second Elevation file, and launched in QGIS and modified using SAGA tool. The drainage channel, stream network or catchment area, basin analysis were done using the processed DEM and the DEM was filled using the Wang and Liu tool under terrain analysis hydrology. The stream network was created using Shrahler order in SAGA analysis tool. Figure 6 showed the processed DEM, hill shade, slope and aspect maps of the study area. The DEM map showed variation of low and highlands, the highlands are trending in northwest – southeast direction. The higher elevations are generally remarkable across the area (Figure 5a), while larger uplands/hills are noticeable on the hill shade (Figure 5b). Noticeable area of wide space of lowlands are observed in southwestern, and northwestern parts. This implies that there possibility of movement of water towards these locations (discharge area), while highlands/uplands forming the watershed. The slope is generally uniform varying from 6.5 to 89.9 degrees (Figure 5c). The aspect which is the direction of the slope from 39 to 359 degrees (Figure 5d).

The drainage network and catchment area is shown in Figure 6. The area is well drained by few river channels (Figure 6a), with large catchment especially at the northern part (Figure 6b). The drainage basin fall with the low basin (Figure 7a) with generally low flow direction (Figure 7b), and low flow connectivity (Figure 7c).

2. Materials and Methods

Water resource management and planning are critical components of a nation's economic and social growth. Hydrogeological prospecting typically entails the creation of hydrogeological maps, the chemical analysis of water, the drilling of wells/boreholes, observation of the water table, the delineation of groundwater bodies, and the determination of their type through pumping tests (Bell, 2007; Brassington, 1988; Asaad et al., 2004). Figure 8 depicts the data acquisition map, while the techniques used in this research are as follows:

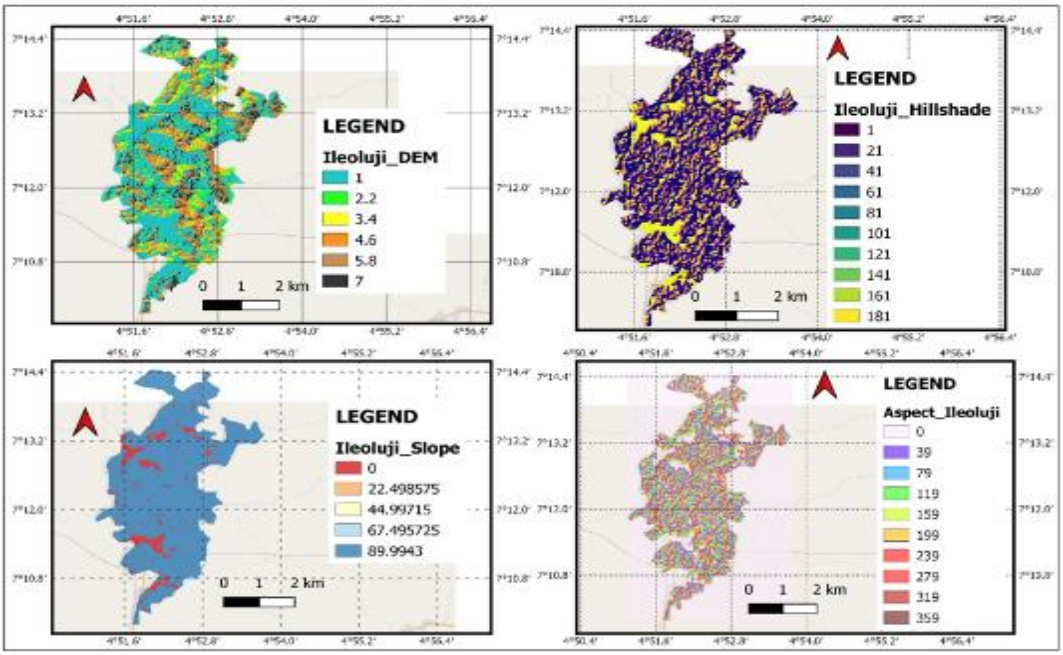

Figure 5: Maps of the digital elevation model (DEM), hill shade, slope, and aspect developed from Quantum geographic information system for the study area

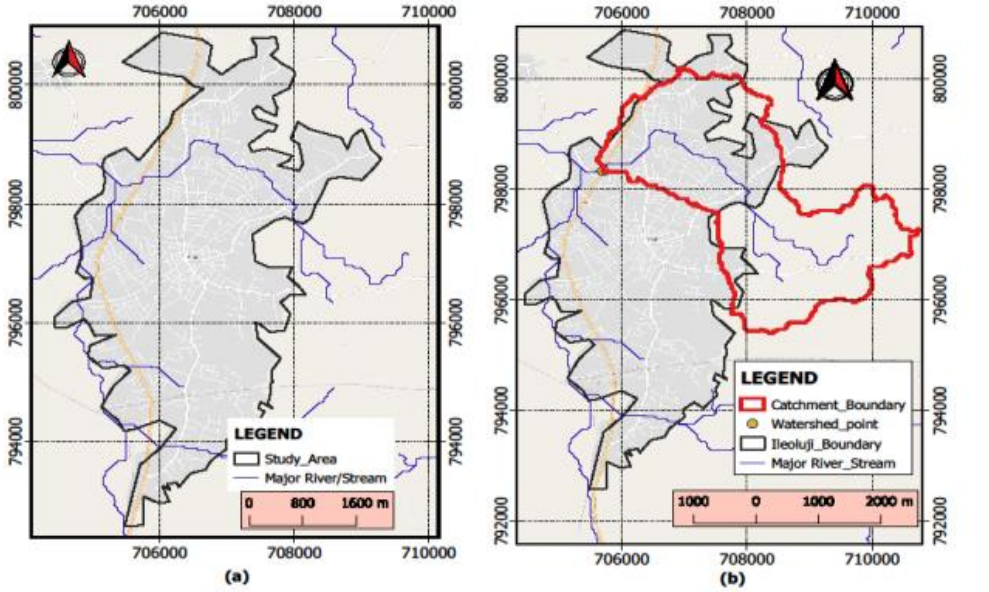

Figure 6: Maps showing the (a) drainage network (b) catchment boundaries for two catchment points at the northern and southern parts

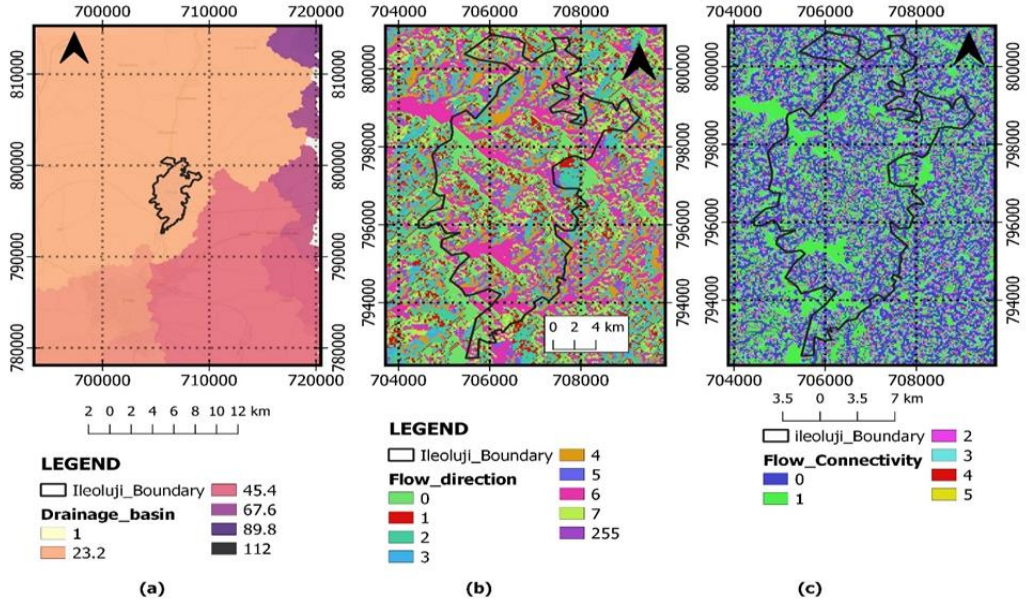

Figure 7: Maps showing the study area's (a) drainage basin type (b) degree of its flow connectivity (c) flow direction

2.1 Direct Investigation

This involved geological mapping of outcrops, geomorphology of the area, and groundwater level measurement/pumping test in wells/boreholes. Boreholes drilling was carried out to examine the lithology by sampling, grain porosity, permeability, thickness, and determination of hydrogeological parameters such as transmissivity, and hydraulic conductivity (Gogoi, 2013; Halford et al., 2006; Johnson, 2005). The geology of the area was the major criterion that was considered or determined the number of boreholes that was drilled and location. The hydrogeological investigation includes static water level and hydraulic head determination from fifty eight open wells across all geological units in the area.

Groundwater levels in fifty eight water wells were monitored early in the morning before abstraction, and the results were used to compute hydraulic heads. The rate of abstraction, operation time/season, depth, and locations were all noted. The steady water level, hydraulic head, borehole depth, water column thickness, and other measurements were taken using a geographic positioning system and steel tape with the lower end marked with carpenter's chalk to allow readings to be taken from the immersed section. To guarantee accuracy, two measurements were obtained at each well/borehole site, and the average values were calculated whenever there was a difference. The readings were used to calculate the thickness of the vadose zone across the region because the depth to the static water level is deemed an estimate of the interface between the vadose and phreatic zones in a non-confined aquifer environment.

Hydraulic parameters from pumping was used to determine the rate of flow, drawdown, transmissivity and storativity (Gogoi, 2013; Halford et al., 2006; Johnson, 2005; Adeleke et al., 2015). The test was carried out in January 2023. The distance from the pumping wells varies from 15 to 50 m and conducted between 1 to 6 hours at pumping rate of 1.125 m^3/day. Before the pumping process started, the initial groundwater level was recorded (h_o) at time t equal to zero, and drawdown were recorded at an interval of 5 min until 120 min when it was observed that further increase in pumping didn't give any corresponding increase in groundwater level, therefore after taking recording at 60 min, the next was taken at 90 min and 120 min, and process terminated and the wells get recharged diffusely and/or localization. There are three methods to replenish a well: spread, indirect, and focused. Diffuse recharge is a form of direct recharge that happens when rainfall percolates through the open zone of the earth to the water table. Small depressions, joints, or cracks can supply concentrated replenishment. Indirect replenishment is provided by mappable features such as rivers, canals, and lakes. The wetted tape method was used to measure total depth, water column height, and static water level. It was inexpensive and simple (but time consuming). To calculate the groundwater elevation, the depth to groundwater was subtracted from the elevation acquired at the surface geo-referenced point.

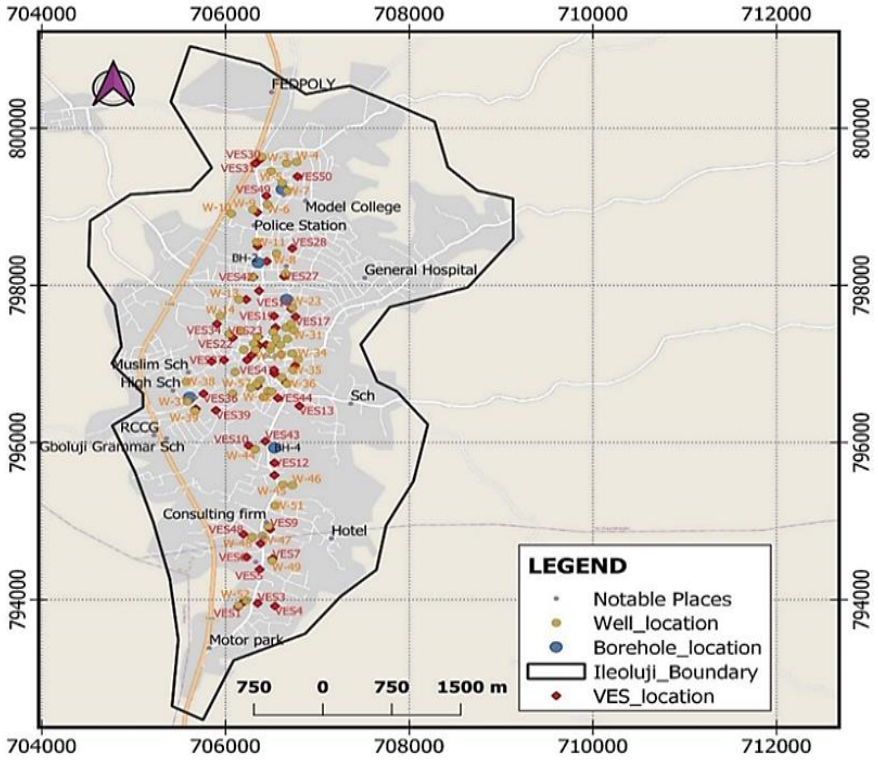

Figure 8: Data acquisition map for the study showing different locations where data were collected from the wells, VESs, and boreholes

2.2 Indirect Investigation

This method encompasses geoelectric methods, the Ohmega resistivity meter was used to conduct the electrical resistivity survey technique using the VES method. Fifty VES points were collected using the Schlumberger electrode setup, with half-current electrode separations varying from 1 m to 150 m. The perceived resistivity values measured were the combination of the resistance received from the resistivity meter and a geometrical component based on the electrode spacing used. The obtained data were plotted against half electrode spacing on a bi-logarithmic graph sheet, and then submitted to partial curve matching and computer iterative modeling (1-D forward modeling) with resist software. Information from existing boreholes was utilized for correlation with the VES data. From the results of the VES, the reflection coefficient (Rc; equation 1), fracture contrast (Fc; equation 2), traverse resistance (T; equation 3), aquifer formation factor (F_M; equation 4) were determined to assess the potentiality of the aquifer system in the area. Longitudinal unit conductance (LC; equation 5) and thickness of the vadose zone determined from the wells were used to determine the vulnerability of aquifer to pollution.

$$Rc = \frac{(\rho_n - \rho)(n-1)}{\rho_n + \rho(n-1)} \quad (1)$$

$$F_c = \frac{\rho_n}{\rho_n - 1} \quad (2)$$

$$T = \sum_{i=1}^{n} \rho_i h_i \quad (3)$$

$$AFM = \frac{average\ aquifer\ water\ \ resistivity}{resistivity\ of\ water\ at\ site} \quad (4)$$

$$LC = \sum_i^n \frac{h_i}{\rho_i} \quad (5)$$

where R_c is reflection coefficient, ρ_n is the layer resistivity of the n^{th} layer, $\rho(n-1)$ is the layer resistivity overlying the n^{th} layer, T is traverse resistance, ρ and h are resistivity and thickness of the nth layer respectively, h_i and ρ_i are the thickness and resistivity of n^{th} layer respectively. The longitudinal resistivity (ρ_l), transverse resistivity (ρ_t), and coefficient of anisotropy (λ) are used in assessing overall aquifer potentiality (Olatunji et al., 2022) using geoelectrical parameters of resistivity and thickness, hence equations 6 and 8 were used.

$$\rho_l = \sum_i^n \frac{h_i}{S_i} \quad (6)$$

$$\rho_t = \sum_i^n \frac{T_i}{h_i} \quad (9)$$

$$\lambda = \sqrt{\frac{\rho_t}{\rho_l}} \quad (10)$$

3. Results and Discussion

3.1 Indirect Method

The summary of the VES is presented in Table 1, while a typical geologic section prepared for VESs 15, 19, 27, 28, and 45 in SW – NE direction, is shown in Figure 9. The curve types (Figure 10) obtained from the study area varied from three layer curve (H), four layer curves (KH, HK, and QH), and five layer curve (HKH), and six layer curve (KHKH). The H curve type is the most preponderant (34 %) followed by KH (24 %), HKH (14 %), QH (14 %), HK (8 %), KHKH (6 %). This implies that the area is generally made of high resistive topsoil, underlain by high conductive weathered layer, and basement rock. These curve types are prolific curve types that suggest subsurface geoelectric configurations apparently favorable for groundwater occurrence, especially in the Basement Complex of Nigeria (Falowo and Daramola, 2023; Bayewu et al., 2018; Akanbi, 2016; Gao et al., 2018).

From the Table 1, topsoil has resistivity ranging from 82 – 652 ohm-m (avg. 279 ohm-m) and thickness varying from 0.5 – 1.5 m (avg. 0.97 m) and composed of clay, sandy clay and clayey sand. The subsoil is characterized with resistivity ranging from 53 – 589 ohm-m (avg. 265 ohm-m) and have same composition as the topsoil, with thickness ranging from 2.1 to 10.5 m (avg. 5.20 m). The weathered layer has resistivity ranging between 38 ohm-m and 751 ohm-m (avg. 212 ohm-m), while resistivity range of 145 – 163 ohm-m is the most widespread (Figure 11a) denoting sandy clay water bearing unit, and resistivity in the range of 38 – 145 ohm-m is extensive in the central and north eastern parts. These indicated a sandy clay weathered layer; the thickness ranged from 4.6 m and 38.7 m (avg. 17.5 m); while the spatial distribution map (Figure 11b) showed thickness range of 10 – 17 m being preponderant. The fractured basement/partly weathered/fresh basement has resistivity of 338 – 6550 ohm-m (avg. 1435 ohm-m), the depths to this rock varied from 9.9 – 39.6 m (avg. 22.4 m). Of the total number of fractured aquifer delineated (20 %), the migmatite recorded 20 %, granite 10 %, and gneiss 70 %. Consequently, the topsoil, subsoil, and weathered layer are generally composed of sandy clay material, which formed the overburden can be regarded as an aquitard. Typical section shown in Figure 6 are characterized by topsoil (99 – 199 ohm-m), subsoil (302 – 413 ohm-m), weathered layer (84 – 251 ohm-m), fractured basement/partly weathered/fresh basement (398 – 3212 ohm-m). The relief of the basement is rugged.

Table 1: VES Interpretation Results

East	North	Elev. (m)	VES NO.	Resistivity (Ohms-meter)						Thickness (m)					Depth (m)					Curve Type
				ρ_1	ρ_2	ρ_3	ρ_4	ρ_5	ρ_6	h_1	h_2	h_3	h_4	h_5	d_1	d_2	d_3	d_4	d_5	
706136	793908	256	1	458	201	1210				1.0	18.5				1	19.5				H
706199	793972	257	2	652	229	1003				0.6	16.5				0.6	17.1				H
706350	793953	256	3	428	112	994				0.8	22.6				0.8	23.4				H
706539	793917	259	4	329	85	778				0.8	17.9				0.8	18.7				H
706371	794384	266	5	201	470	110	885			1.1	5.9	29.5			1.1	7	36.5			KH
706230	794540	266	6	145	351	82	751			0.9	3.9	19.8			0.9	4.8	24.6			KH
706512	794521	267	7	102	315	108	898	217	1023	1.2	3.7	5.9	9.9	14.7	1.2	4.9	10.8	20.7	35.4	KHKH
706382	794714	266	8	551	99	614	225	898		0.8	6.3	4.6	18.1		0.8	7.1	11.7	29.8		HKH
706486	794897	260	9	361	523	188	858	91	1223	0.9	2.8	10.5	6.8	17.3	0.9	3.7	14.2	21	38.3	KHKH
706251	795960	262	10	233	357	65	1425			0.9	2.3	27.2			0.9	3.2	30.4			KH
706533	795584	264	11	189	421	147	1236			1.3	4.1	17.0			1.3	5.4	22.4			KH
706533	795740	265	12	345	72	1101				1.1	18.7				1.1	19.8				H
706805	796464	254	13	312	65	568				0.8	22.6				0.8	23.4				H
706659	796757	263	14	82	53	38	655			0.5	3.3	12.3			0.5	3.8	16.1			QH
706444	797243	259	15	99	413	118	3212			0.9	5.6	26.8			0.9	6.5	33.3			KH
706544	797462	252	16	128	520	213	1002			1.0	10.5	19.2			1	11.5	30.7			KH
706763	797600	256	17	241	158	92	998			1.2	5.7	14.4			1.2	6.9	21.3			QH
706716	797701	256	18	305	193	102	689			1.2	6.3	17.9			1.2	7.5	25.4			QH
706528	797609	252	19	187	410	251	1356			0.6	4.0	13.5			0.6	4.6	18.1			KH
706288	797114	268	20	201	88	806				0.9	20.5				0.9	21.4				H
706235	797050	269	21	362	132	1455				0.8	16.8				0.8	17.6				H
706079	797334	257	22	446	144	521	97	936		0.8	2.1	9.8	16.2		0.8	2.9	12.7	28.9		HKH
706356	797343	252	23	354	222	751	123	1330		0.9	3.3	12.3	15.7		0.9	4.2	16.5	32.2		HKH
706361	797233	262	24	319	195	470	122	1114		0.9	2.9	7.7	16.8		0.9	3.8	11.5	28.3		HKH
706366	797930	259	25	229	87	999				0.8	23.2				0.8	24				H
706225	797820	255	26	310	45	1652				1.2	16.5				1.2	17.7				H
706638	798113	264	27	199	84	2356				1.4	18.7				1.4	20.1				H
706727	**798470**	263	28	175	302	201	852			1.1	6.3	18.9			1.1	7.4	26.3			KH
706450	798305	267	29	502	322	612	108	1232		0.9	3.8	10.3	14.8		0.9	4.7	15	29.8		HKH
706382	799606	272	30	156	98	57	911			0.6	6.9	18.5			0.6	7.5	26			QH
706324	799551	269	31	195	120	68	1102			0.9	7.1	19.6			0.9	8	27.6			QH
706345	798928	260	32	314	132	458	110	2250		1.2	2.5	8.9	19.4		1.2	3.7	12.6	32		HKH
706350	798498	258	33	445	80	2378				1.1	18.2				1.1	19.3				H
705906	797508	255	34	329	89	1468				1.3	23.4				1.3	24.7				H
705613	796537	258	35	498	120	877				0.9	22.2				0.9	23.1				H
705760	796620	259	36	214	403	182	2444			1.1	7.4	18.3			1.1	8.5	26.8			KH

Table 1: Continued

Table 1: VES Interpretation Results																			
East	North	Elev. (m)	VES NO.	Resistivity (Ohmns-meter)						Thickness (m)					Depth (m)					Curve Type
				ρ_1	ρ_2	ρ_3	ρ_4	ρ_5	ρ_6	h_1	h_2	h_3	h_4	h_5	d_1	d_2	d_3	d_4	d_5	
705984	797050	261	37	205	81	801				0.8	22.5				0.8	23.3				H
705849	797032	258	38	222	419	90	3358			1.4	5.4	19.2			1.4	6.8	26			KH
705896	796409	259	39	474	221	6550				0.5	15.5				0.5	16				H
705676	796427	258	40	188	369	102	1616			0.8	3.4	13.7			0.8	4.2	17.9			KH
706758	796977	266	41	112	589	174	4122			1.5	2.2	9.8			1.5	3.7	13.5			KH
706303	798104	265	42	477	214	509	115	2750		1.1	8.8	19.4			1.1	9.9	29.3			HKH
706434	796015	261	43	94	218	144	998	58	3696	1.3	7.7	12.3	8.2	13.8	1.3	9	21.3	29.5	43.3	KHKH
706570	796565	258	44	232	152	93	750			0.7	6.9	18.6			0.7	7.6	26.2			QH
706350	796720	267	45	168	85	445	398			0.9	6.9	13.4			0.9	7.8	21.2			HK
706533	796876	274	46	86	45	690				0.9	38.7				0.9	39.6				H
706528	796922	274	47	314	112	555	410			1.1	9.9	19.2			1.1	11	30.2			HK
706194	794833	262	48	186	92	480	338			1.2	5.4	18.7			1.2	6.6	25.3			HK
706444	799139	267	49	411	147	621	448			1.2	3.6	14.9			1.2	4.8	19.7			HK
706784	799386	269	50	159	121	94	661			0.8	3.3	21.2			0.8	4.1	25.3			QH

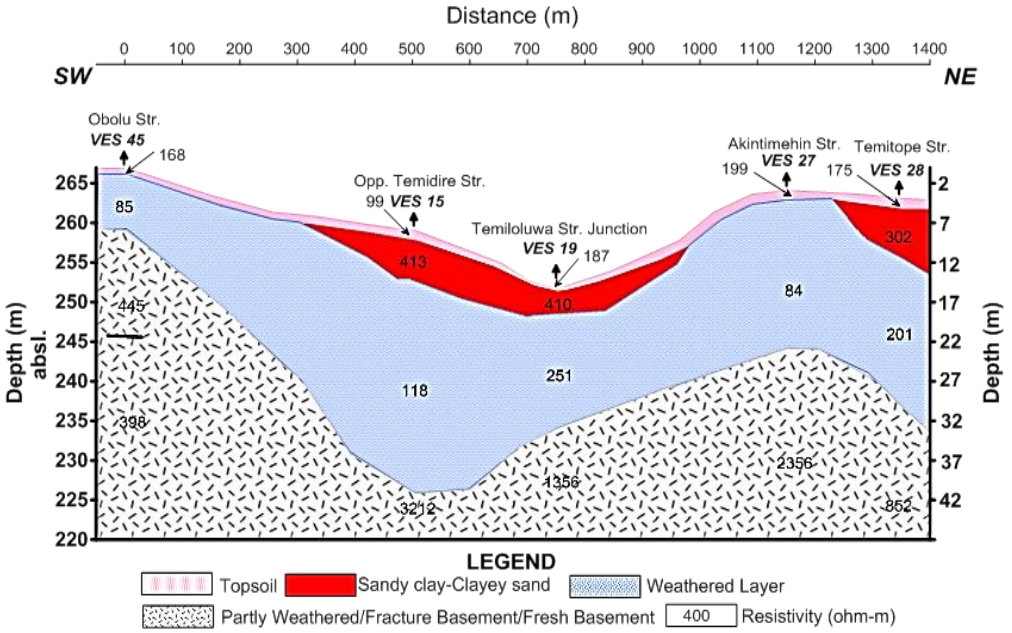

Figure 9: Geologic Section/Profile along the selected VES point established in the study area

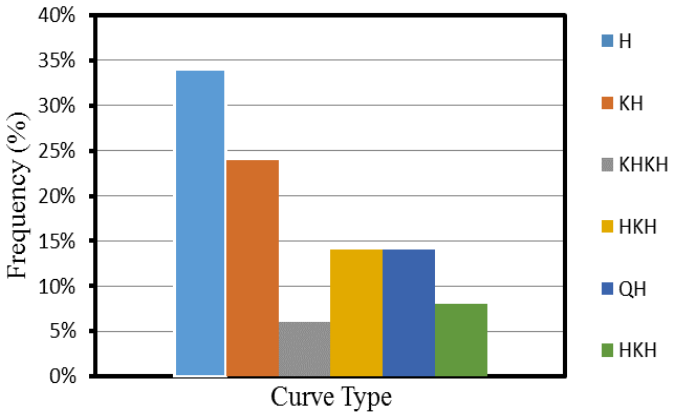

Figure 10: The frequency chart of the obtained Curve Types

The overburden thickness of the study area ranged from 13.5 – 43.3 m with regional average of 25.3 m, with migmatite, granite, and gneiss, recorded averages of 24.3 m, 24.5 m, and 27.9 m respectively; hence the overburden thickness is relatively higher in granite gneiss environment. The spatial variation of the overburden thickness is shown in Figure 11c, overburden thickness in the range of 13.5 to 24.1 m is the most dominant, which can regarded as moderate/thick weathering profile. In the basement complex of southwestern Nigeria, overburden thickness above 15 m is usually considered thick and prolific for groundwater accumulation, hence the study area is highly favourable to groundwater propensity. Therefore priority most be given to those zones during groundwater development scheme in the area. Although the nature of the overburden in terms of resistivity, transmissivity, hydraulic conductivity, and hydraulic gradient are also important parameters in deciphering overall water yield of the weathered layer (Falowo et al., 2020).

Table 2 showed the data calculated for aquifers' units' characteristics, hydraulic characteristics, and longitudinal unit conductance values for the study area. The geology of the area where the VESs were conducted are migmatite (constitutes 32 % of the VES area), granite (42 %), and gneiss (25 %), with the weathered layer (80%) being the major aquifer, and fractured basement (20 %) is the minor aquifer. The estimated formation factor (F_M) ranged from 1.79 (granite) – 1.96 (gneiss) - 3.50 (migmatite) and average value of 2.38. Formation factor has good positive correlation with groundwater yield, therefore migmatite showed better tendency. Figure 12a showed low F_M across the area (less than 10), however relatively high are common in the southern part, and low values in the northern part. This indicates low groundwater yield according to Table 8. The estimated hydraulic conductivity (K) obtained ranged from 0.22 – 0.55 m/d (0.37 m/d) which suggests clay sand and corroborates the VES result; while the geological units recorded: migmatite (0.22 – 0.55 m/d; 0.39 m/d avg.), granite (0.26 – 0.42 m/d; 0.35 m/d avg.), and gneiss (0.25 – 0.51 m/d; 0.36 m/d avg. The transmissivity (T) varied between 3.49 to 15.61 m^2/d (6.86 m^2/d avg.), while the respective geologic units ranged from migmatite: 4.13 – 10.21 m^2/d (7.17 m^2/d avg.), granite: 3.49 – 15.61 m^2/d (7.14 m^2/d avg.), and gneiss: 3.80 – 9.20 m^2/d (6.02 m^2/d avg.). The spatial distribution of K and T in Figure 12b & c showed general values of K in the range of 0.35 to 0.38 m/d; while T distinguished the area into two zones i.e. zone with T greater than 10 (in central and northwester parts) and southern and northeastern part where Tis less than 10. However using the criteria in Table 8, the average T value fall within low group since the values are less than 10 m^2/d.

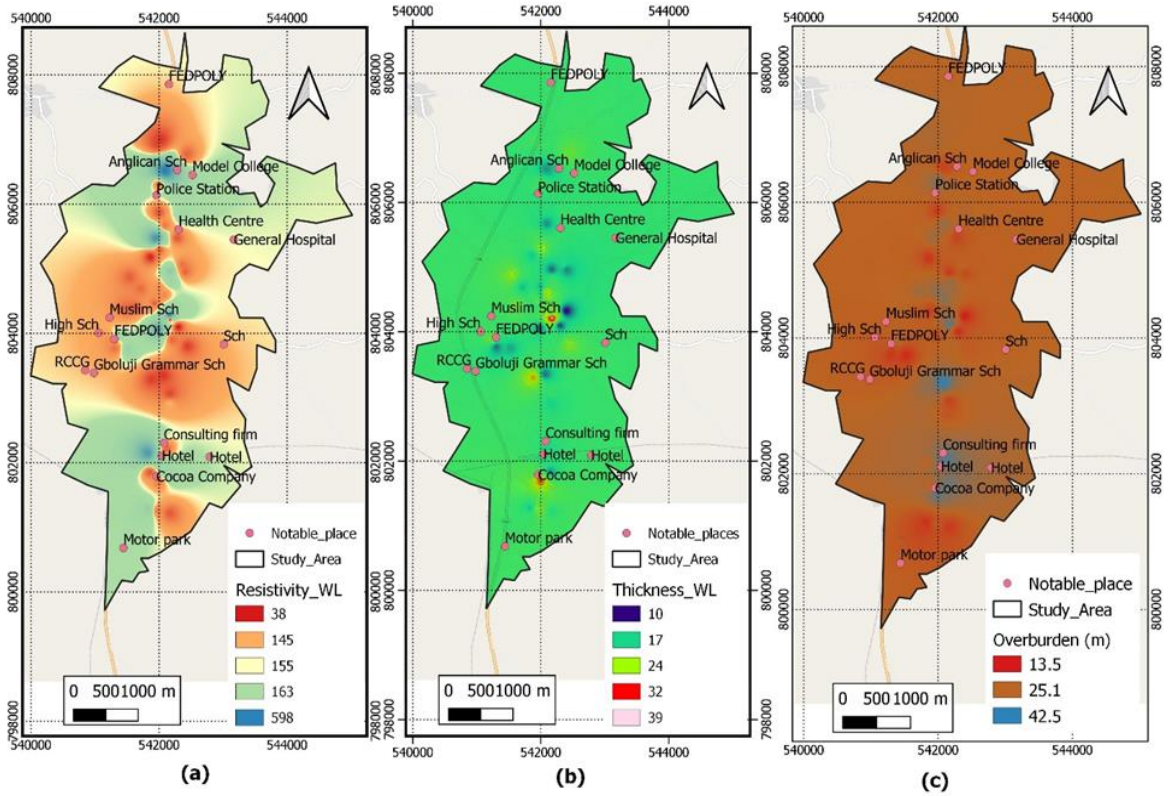

Figure 11: Spatial Distribution Map of (a) Resistivity of the weathered layer (b) Thickness of the weathered layer (c) Overburden thickness across the study area

The fracture contrast and reflection coefficient ranged between 0.18 – 63.72 (12.97 avg.) and -0.17 to 0.97 (0.747 avg.). The average FC and RC values obtained for migmatite are 8.34 and 0.62; granite: 14.23 and 0.79; gneiss: 16.64 and 0.83. The fracture contrast and reflection coefficient have strong relationship with groundwater yield, as high FC implies high groundwater potential; and low RC indicates high groundwater yield. The spatial distribution map of RC and FC is shown in Figure 13, the RC and FC values in the range of 0.6850 – 0.9699 (Figure 13a) and 2.93 to 61.07 (Figure 13b) are the most prominent, although relatively high values of FC and low values of RC are seen at sporadic spots in each of the southern, central, and northern parts. These spotted locations are high groundwater yield or propensity zones characterized with weathered or partly weathered/fracture basement groundwater saturated aquifer. The transverse (P_T) and longitudinal (P_L) resistivity ranged from 42.44 – 521.59 (191.93 avg.) and 41.07 – 383.25 (148.0 avg.) respectively, while the geologic units recorded average values of 211.22 and 165.29 (migmatite); 157.38 and 128.95 (granite); and 224.0 and 157.50 (gneiss). The Zordy coefficient of anisotropy or electrical anisotropy (λ) ranged between 1 and 1.55 (avg. 1.12); while averages of 1.11, 1.09, and 1.19 were recorded for migmatite, granite, and gneiss respectively, and from all these results, the gneiss showed best groundwater prolificacy.

Table 2: Summary of aquifer units' characteristics, hydraulics characteristics, derived geoelectric properties, and vulnerability

VES No.	Aquifer Unit				Overburden Thickness (m)	S (⍰$^{-1}$)	T (⍰m^2)	K (m/day)	T (m^2/day)	Fc	Rc	Fm	PT	PL	λ
	Resistivity (Ωm)	Thickness (m)	Geology	Type											
1	201	18.5	Migmatite	Weathered Layer	19.5	0.0942	4177	0.55	10.21	6.02	0.72	3.50	214.18	206.96	1.02
2	229	16.5	Migmatite	Weathered Layer	17.1	0.0730	4170	0.25	4.13	4.38	0.63	3.50	243.84	234.33	1.02
3	112	22.6	Migmatite	Weathered Layer	23.4	0.2037	2874	0.22	4.97	8.88	0.80	3.50	122.80	114.90	1.03
4	85	17.9	Granite	Weathered Layer	18.7	0.2130	1785	0.26	4.65	9.15	0.80	1.79	95.44	87.79	1.04
5	110	29.5	Granite	Weathered Layer	36.5	0.2862	6239	0.41	12.23	8.05	0.78	1.79	170.93	127.53	1.16
6	82	19.8	Granite gneiss	Weathered Layer	24.6	0.2588	3123	0.25	5.02	9.16	0.80	1.96	126.95	95.06	1.16
7	217	14.7	Granite gneiss	Fracture Aquifer	35.4	0.1569	14005	0.26	3.80	4.71	0.65	1.96	305.52	225.61	1.16
8	225	18.1	Granite gneiss	Fracture Aquifer	29.8	0.1530	7961	0.26	4.77	0.37	0.60	1.96	267.16	194.74	1.17
9	91	17.3	Migmatite	Fracture Aquifer	38.3	0.2617	11172	0.55	9.55	13.44	0.86	3.50	250.59	146.33	1.31
10	65	27.2	Granite gneiss	Weathered Layer	30.4	0.4288	2799	0.27	7.30	21.92	0.91	1.96	92.07	70.90	1.14
11	147	17	Migmatite	Weathered Layer	22.4	0.1323	4471	0.27	4.65	8.41	0.79	3.50	199.59	169.36	1.09
12	72	18.7	Granite	Weathered Layer	19.8	0.2629	1726	0.28	5.20	15.29	0.88	1.79	87.17	75.31	1.08
13	65	22.6	Granite	Weathered Layer	23.4	0.3503	1719	0.41	9.37	8.74	0.79	1.79	73.44	66.81	1.05
14	38	12.3	Granite	Weathered Layer	16.1	0.3920	683	0.28	3.49	17.24	0.89	1.79	42.44	41.07	1.02
15	118	26.8	Granite	Weathered Layer	33.3	0.2498	5564	0.29	7.73	27.22	0.93	1.79	167.10	133.32	1.12
16	213	19.2	Granite	Weathered Layer	30.7	0.1181	9678	0.29	5.63	4.70	0.65	1.79	315.23	259.85	1.10
17	92	14.4	Granite gneiss	Fracture Aquifer	21.3	0.1976	2515	0.51	7.28	10.85	0.83	1.96	118.06	107.81	1.05
18	102	17.9	Granite	Weathered Layer	25.4	0.2121	3408	0.30	5.34	6.75	0.74	1.79	134.16	119.77	1.06
19	251	13.5	Granite	Weathered Layer	18.1	0.0667	5141	0.30	4.10	5.40	0.69	1.79	284.02	271.16	1.02
20	88	20.5	Migmatite	Weathered Layer	21.4	0.2374	1985	0.31	6.32	9.16	0.80	3.50	92.75	90.13	1.01
21	132	16.8	Migmatite	Weathered Layer	17.6	0.1295	2507	0.55	9.28	11.02	0.83	3.50	142.45	135.93	1.02
22	97	16.2	Granite gneiss	Fracture Aquifer	28.9	0.2022	7336	0.31	5.08	0.19	0.81	1.96	253.85	142.93	1.33
23	123	15.7	Granite gneiss	Fracture Aquifer	32.2	0.1614	12220	0.32	5.00	10.81	0.83	1.96	379.49	199.47	1.38
24	122	16.8	Granite gneiss	Fracture Aquifer	28.3	0.1718	6521	0.32	5.43	9.13	0.80	1.96	230.43	164.74	1.18
25	87	23.2	Granite	Weathered Layer	24	0.2702	2202	0.41	9.62	11.48	0.84	1.79	91.73	88.84	1.02
26	45	16.5	Granite	Weathered Layer	17.7	0.3705	1115	0.33	5.42	36.71	0.95	1.79	62.97	47.77	1.15
27	84	18.7	Migmatite	Weathered Layer	20.1	0.2297	1849	0.33	6.23	28.05	0.93	3.50	92.01	87.52	1.03
28	201	18.9	Migmatite	Weathered Layer	26.3	0.1212	5894	0.34	6.39	4.24	0.62	3.50	224.11	217.04	1.02

Table 2: Continued

Table 2: Summary of aquifer units' characteristics, hydraulics characteristics, derived geoelectric properties, and vulnerability

VES No.	Aquifer Unit				Overburden Thickness (m)	S (Ω^{-1})	T (Ωm^2)	K (m/day)	T (m^2/day)	Fc	Rc	F_M	PT	PL	λ
	Resistivity (Ωm)	Thickness (m)	Geology	Type											
29	108	14.8	Granite	Fracture Aquifer	29.8	0.1675	9577	0.39	5.79	0.18	0.84	1.79	321.39	177.95	1.34
30	57	18.5	Granite	Weathered Layer	26	0.3988	1824	0.34	6.35	15.98	0.88	1.79	70.17	65.19	1.04
31	68	19.6	Granite	Weathered Layer	27.6	0.3520	2360	0.35	6.83	16.21	0.88	1.79	85.52	78.41	1.04
32	110	19.4	Migmatite	Fracture Aquifer	32	0.2186	6917	0.35	6.85	0.24	0.91	3.50	216.16	146.41	1.22
33	80	18.2	Granite gneiss	Weathered Layer	19.3	0.2300	1946	0.51	9.20	29.73	0.93	1.96	100.80	83.92	1.10
34	89	23.4	Migmatite	Weathered Layer	24.7	0.2669	2510	0.36	8.38	16.49	0.89	3.50	101.63	92.55	1.05
35	120	22.2	Migmatite	Weathered Layer	23.1	0.1868	3112	0.36	8.07	7.31	0.76	3.50	134.73	123.66	1.04
36	182	18.3	Migmatite	Weathered Layer	26.8	0.1241	6548	0.37	6.74	13.43	0.86	3.50	244.34	216.04	1.06
37	81	22.5	Granite	Weathered Layer	23.3	0.2817	1987	0.41	9.33	9.89	0.82	1.79	85.26	82.72	1.02
38	90	19.2	Granite	Weathered Layer	26	0.2325	4301	0.37	7.17	37.31	0.95	1.79	165.44	111.81	1.22
39	221	15.5	Granite	Weathered Layer	16	0.0712	3663	0.38	5.86	29.64	0.93	1.79	228.91	224.75	1.01
40	102	13.7	Granite	Weathered Layer	17.9	0.1478	2802	0.38	5.25	15.84	0.88	1.79	156.56	121.12	1.14
41	174	9.8	Granite gneiss	Weathered Layer	13.5	0.0734	3169	0.51	4.95	23.69	0.92	1.96	234.74	183.80	1.13
42	509	19.4	Granite gneiss	Weathered Layer	29.3	0.0815	12283	0.39	7.53	23.91	0.92	1.96	419.20	359.33	1.08
43	58	13.8	Granite gneiss	Fracture Aquifer	43.3	0.3807	12556	0.39	5.43	63.72	0.97	1.96	271.49	113.73	1.55
44	93	18.6	Granite gneiss	Weathered Layer	26.2	0.2484	2941	0.40	7.41	8.06	0.78	1.96	112.25	105.47	1.03
45	445	13.4	Migmatite	Weathered Layer	21.2	0.1166	6701	0.55	7.40	0.89	-0.06	3.50	316.07	181.75	1.32
46	45	38.7	Granite	Weathered Layer	39.6	0.8705	1819	0.40	15.61	15.33	0.88	1.79	45.93	45.49	1.00
47	555	19.2	Migmatite	Weathered Layer	30.2	0.1265	12110	0.41	7.84	0.74	-0.15	3.50	401.00	238.75	1.30
48	480	18.7	Migmatite	Weathered Layer	25.3	0.1041	9696	0.41	7.73	0.70	-0.17	3.50	383.24	243.02	1.26
49	621	14.9	Granite	Weathered Layer	19.7	0.0514	10275	0.41	6.18	0.72	-0.16	1.79	521.59	383.25	1.17
50	94	21.2	Granite	Weathered Layer	25.3	0.2578	2519	0.42	8.87	7.03	0.75	1.79	99.58	98.12	1.01

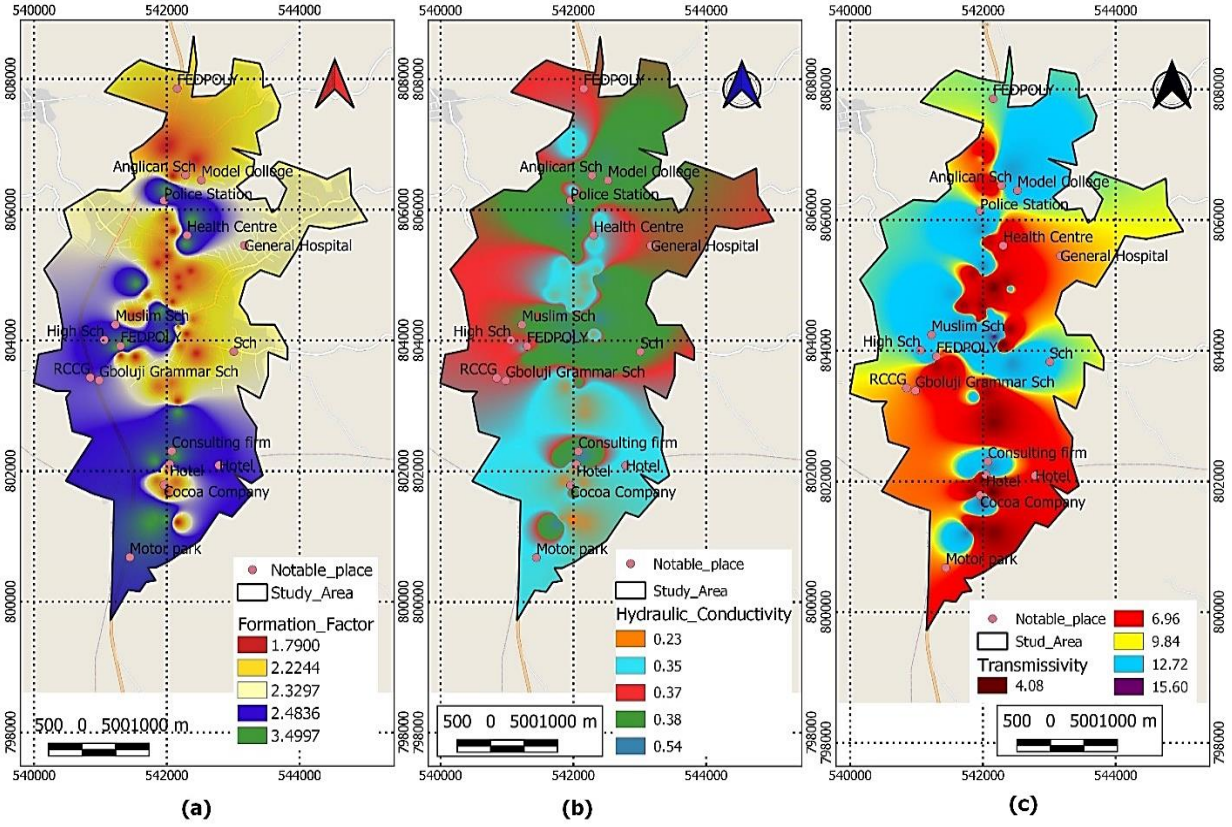

Figure 12: Spatial map of (a) Formation factor (b) Hydraulic conductivity (c) Transmissivity across the study area

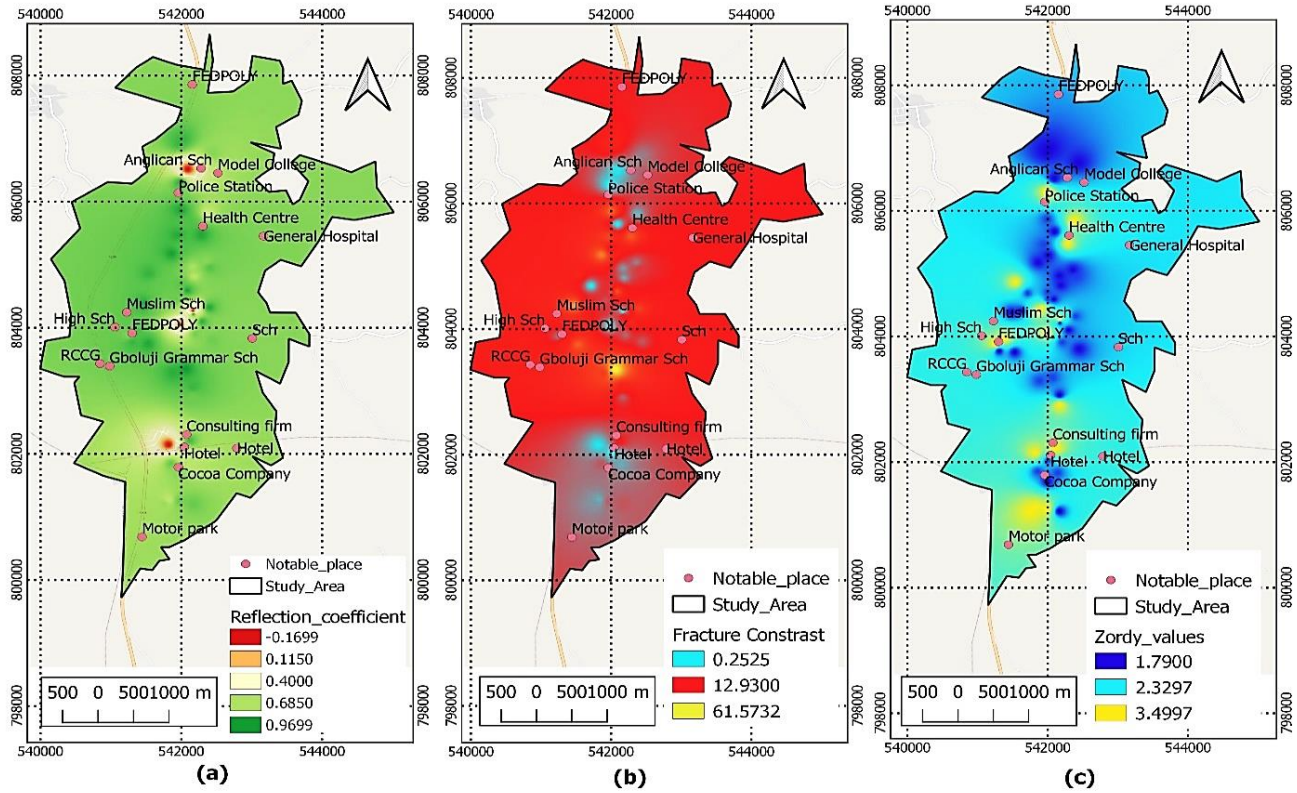

Figure 13: Spatial distribution map of (a) Reflection coefficient (b) Fracture contrast (c) Coefficient of Anisotropy across the study area

The traverse resistance ranged from 683 - 14005 Ωm² (avg. 5129 Ωm²). The average values estimated for different geological units in the area: migmatite, granite, and gneiss are 5418 Ωm², 3828 Ωm², and 6875 Ωm² respectively with gneiss having the highest value (Table 2). The spatial transverse resistance values are shown in Figure 14a, lower values less than 5000 ohm-m² are areas with low yield/potential, values ranging from 5000 – 10000 ohm-m² are moderate groundwater potential area, while values above 10000 are high prospect zones. Hence the area range from low – moderate in equal proportion by areal extent. Aquifer transmissivity and traverse resistance have recorded positive correlation coefficient, hence transmissivity increases as the transverse resistance increases (Falowo, 2022). Consequently, the north central and portion of mid southern part showed moderate tendency.

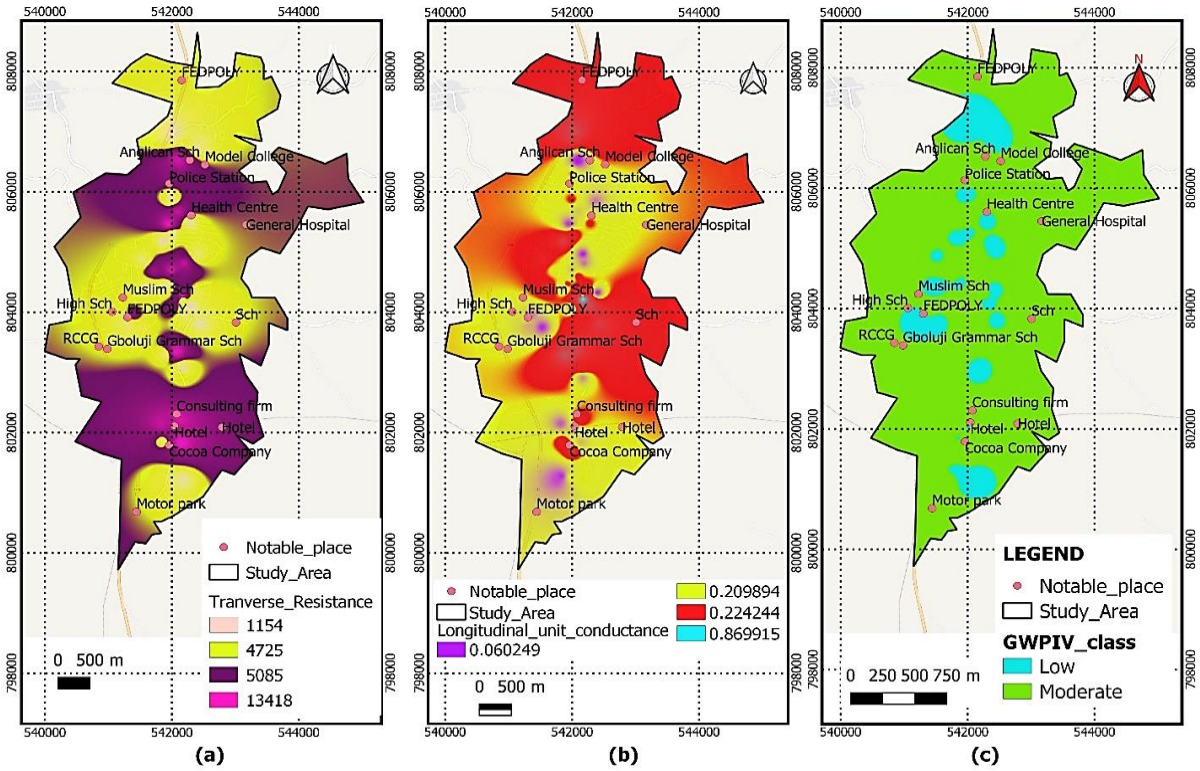

Figure 14: Distribution of (a) Transverse resistance (b) Longitudinal unit conductance (c) Groundwater potential index values

Table 3: Summary of Well Information and Sample Locations

East (m)	North (m)	Borehole No.	Elevation (m)	Total Depth (m)	SWL (m)	Geology	Present State
706617	799222	BH-1	267	38	22	Migmatite	Functioning
706356	798287	BH-2	267	42	19	Granite	Functioning
705608	796574	BH-3	258	45	22	Migmatite	Functioning
706533	795932	BH-4	262	39	20	Gneiss	Functioning
706664	797820	BH-5	257	48	26	Granite-Gneiss	Functioning

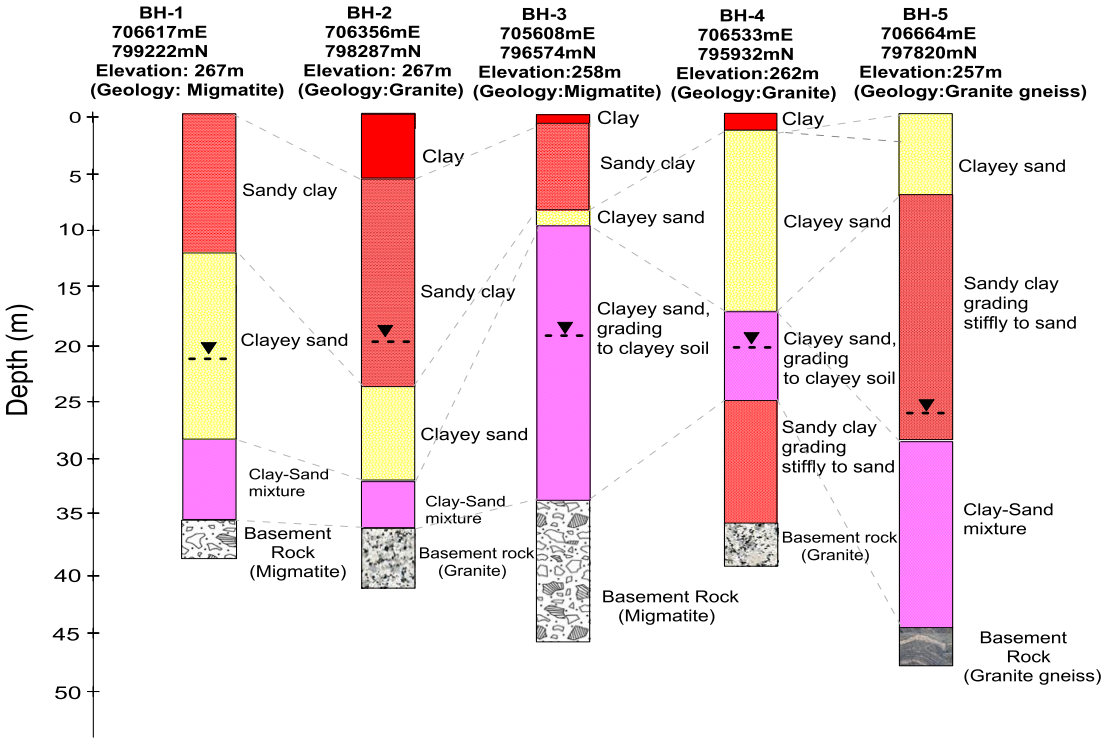

Figure 15: Borehole sections showing the various geologic units observed from borehole cuttings across three geological environments of migmatite, granite, and gneiss

Table 4: Summary of Well Information from two geological units

East	North	Well. No	Elevation (m)	TD (m)	SWL (m)	WC (m)	HH (m)	K (m/day)	T (m^2/day)	Geology
706397	799634	W-1	272	8.2	4.5	3.7	267.5	0.41	1.53	Granite
706497	799451	W-2/VES 49	269	12.3	7.5	4.8	261.5	0.41	1.99	Granite
706664	799551	W-3	271	14.5	8.2	6.3	262.8	0.41	2.61	Granite
706774	799570	W-4/VES50	271	6.5	3.2	3.3	267.8	0.41	1.37	Granite
706617	799304	W-5	268	9.5	5.5	4	262.5	0.41	1.66	Granite
706455	799029	W-6	266	8.7	3.9	4.8	262.1	0.41	1.99	Granite
706674	799203	W-7	267	10.4	6.2	4.2	260.8	0.41	1.74	Granite
706554	798406	W-8	263	12.7	5.8	6.9	257.2	0.41	2.86	Granite
706298	798965	W-9	261	9.8	6.3	3.5	254.7	0.41	1.45	Granite
706063	798910	W-10	258	7.8	4.3	3.5	253.7	0.41	1.45	Granite
706340	798553	W-11	256	13.3	5.6	7.7	250.4	0.41	3.19	Granite
706293	798104	W-12/VES 25	264	15.1	8.2	6.9	255.8	0.41	2.86	Granite
706146	797820	W-13	255	8.6	5.2	3.4	249.8	0.51	1.72	Granite Gneiss
705943	797609	W-14	255	9.5	3.7	5.8	251.3	0.41	2.40	Granite
706037	797380	W-15/VES 37	256	8.2	5.3	2.9	250.7	0.41	1.20	Granite
706162	797417	W-16	254	12.2	6.8	5.4	247.2	0.55	2.98	Migmatite
706350	797343	W-17/VES 20	252	14.6	5.6	9	246.4	0.55	4.97	Migmatite
706309	797261	W-18/VES 21	259	8.8	2.5	6.3	256.5	0.55	3.48	Migmatite
706329	797178	W-19	266	6.7	3.4	3.3	262.6	0.51	1.67	Granite Gneiss
706199	797178	W-20	263	11.3	7.2	4.1	255.8	0.51	2.07	Granite Gneiss
706654	798150	W-21	265	14.9	6.8	8.1	258.2	0.51	4.09	Granite Gneiss
706518	797407	W-22	252	9.2	3.8	5.4	248.2	0.51	2.73	Granite Gneiss
706727	797719	W-23/VES 17	256	8.0	5.5	2.5	250.5	0.51	1.26	Granite Gneiss
706486	797188	W-24	262	11.4	7.4	4	254.6	0.51	2.02	Granite Gneiss
706497	797233	W-25	259	9.6	5.2	4.4	253.8	0.51	2.22	Granite Gneiss
706549	797325	W-26	255	7.4	3.6	3.8	251.4	0.51	1.92	Granite Gneiss
706659	797462	W-27	254	12.8	7.9	4.9	246.1	0.51	2.48	Granite Gneiss
706716	797508	W-28	255	10.9	6.5	4.4	248.5	0.55	2.43	Migmatite
706596	797243	W-29	259	13.3	8.1	5.2	250.9	0.55	2.87	Migmatite
706674	797316	W-30	257	8.5	4.4	4.1	252.6	0.55	2.26	Migmatite
706742	797426	W-31	256	9.9	3.6	6.3	252.4	0.55	3.48	Migmatite
706606	797123	W-32	264	8.7	3.5	5.2	260.5	0.55	2.87	Migmatite
706727	797133	W-33	263	9.2	5.2	4	257.8	0.55	2.21	Migmatite
706789	797059	W-34	263	8.6	4.3	4.3	258.7	0.41	1.78	Granite
706732	796922	W-35/VES 14	268	9.7	6.5	3.2	261.5	0.41	1.33	Granite
706669	796748	W-36	262	10.7	6.9	3.8	255.1	0.41	1.58	Granite
705587	796519	W-37	257	8.7	3.3	5.4	253.7	0.41	2.24	Granite
705571	796775	W-38/VES 35	257	6.5	4.0	2.5	253	0.55	1.38	Migmatite
705666	796400	W-39	257	9.8	4.9	4.9	252.1	0.41	2.03	Granite
706079	796620	W-40	257	10.8	7.2	3.6	249.8	0.41	1.49	Granite
706413	796574	W-41/VES 33	261	7.7	4.6	3.1	256.4	0.51	1.57	Granite Gneiss
706465	796656	W-42	264	9.5	4.8	4.7	259.2	0.41	1.95	Granite
706502	796647	W-43	263	10.5	5.6	4.9	257.4	0.55	2.71	Migmatite
706324	795914	W-44/VES 8	263	12.3	7.7	4.6	255.3	0.55	2.54	Migmatite
706622	795465	W-45/VES 9	265	9.4	6.2	3.2	258.8	0.55	1.77	Migmatite
706727	795456	W-46/VES 32	264	7.6	5.5	2.1	258.5	0.55	1.16	Migmatite
706403	794815	W-47	262	8.9	3.9	5	258.1	0.51	2.53	Granite Gneiss
706288	794796	W-48/VES 6	263	13.8	7.9	5.9	255.1	0.51	2.98	Granite Gneiss
706507	794494	W-49	267	11.5	6.6	4.9	260.4	0.51	2.48	Granite Gneiss
706465	794934	W-50	259	12.6	8.1	4.5	250.9	0.51	2.27	Granite Gneiss

Table 4: Continued

Table 4: Summary of Well Information from two geological units

East	North	Well. No	Elevation (m)	TD (m)	SWL (m)	WC (m)	HH (m)	K (m/day)	T (m^2/day)	Geology
706539	795199	W-51	264	10.2	5.8	4.4	258.2	0.51	2.22	Granite Gneiss
706225	793990	W-52/VES 44	257	8.5	4.7	3.8	252.3	0.51	1.92	Granite Gneiss
706141	793926	W-53	257	8.9	6.2	2.7	250.8	0.51	1.36	Granite Gneiss
706105	796894	W-54	265	9.0	6.1	2.9	258.9	0.51	1.47	Granite Gneiss
706376	796794	W-55	270	8.5	4.2	4.3	265.8	0.51	2.17	Granite Gneiss
706340	796739	W-56	267	10.5	5.9	4.6	261.1	0.51	2.32	Granite Gneiss
706277	796693	W-57	264	8.7	4.7	4	259.3	0.41	1.66	Granite
706612	796830	W-58	270	7.6	3.8	3.8	266.2	0.41	1.58	Granite

3.2 Direct Method

The information from the boreholes is presented in Table 3, with total depth ranging from 38 (migmatite) – 48 m (gneiss) and an average of 42 m, showed SWL ranging from 19 (granite) – 26 m in gneiss (avg. 22.0 m). Hydraulic information was taken from fifty five wells, and some of the wells coincided with the location of the VES's stations, as presented in Tables 5 and 6. This information showed that the area has a thick overburden thickness/depth of weathering and corroborates the obtained geoelectric data i.e. 22.0 m. The sections of the boreholes are presented in Figure 15. The cuttings were visually inspected in their natural state or condition during drilling. The geologic units observed from the sites investigated (within migmatite, granite, and gneiss environments) comprised clay, sandy clay, clayey sand (which graded to sand or clayey material in many places), clay-sand mixture, and fresh basement rock. The thickness of the clay topsoil delineated under BHs-02 – 04 ranged from 1.1 – 5.7 m; the sandy clay was observed in all the boreholes with thickness range of 7.6 m (BH-03) to 23.2 m (BH-05); clayey sand has thickness variation of 1.2 m (BH-03) to 15.5 m (BH-04); clay-sand mixture has thickness varying from 3.3 m (BH-02) to 23.5 m (BH-03). The clay-sand mixture is the main water bearing units, which constitute the weathered layer. The depth to basement rock ranged between 33.8 – 44.1 m. The upper 10 m of the sections are dominated by clay, sandy clay, and clayey sand; while sandy clay being the most dominant soil. The SWL is deep ranging from 18.5 – 24.6 m. The structural features possibly fractures observed in BHs-01, 05, and 06 agreed with the fractured zone delineated on the geoelectric data with depths range of 25 – 38.5 m and average depth of 29.8 m. This range of values overlap and within the 32.0 – 43.5 m delineated in the sections. This zone and weathered layer are the main water bearing units in the area. The depth to the basement ranged from 33.5 m for borehole 03 (migmatite) – 44.4 m for borehole 05 (gneiss). This supports the overburden thickness of 13.5 to 43.3 m recorded in VES results for gneiss. Hence gneissic offered both thick weathered layer and fractured aquifer.

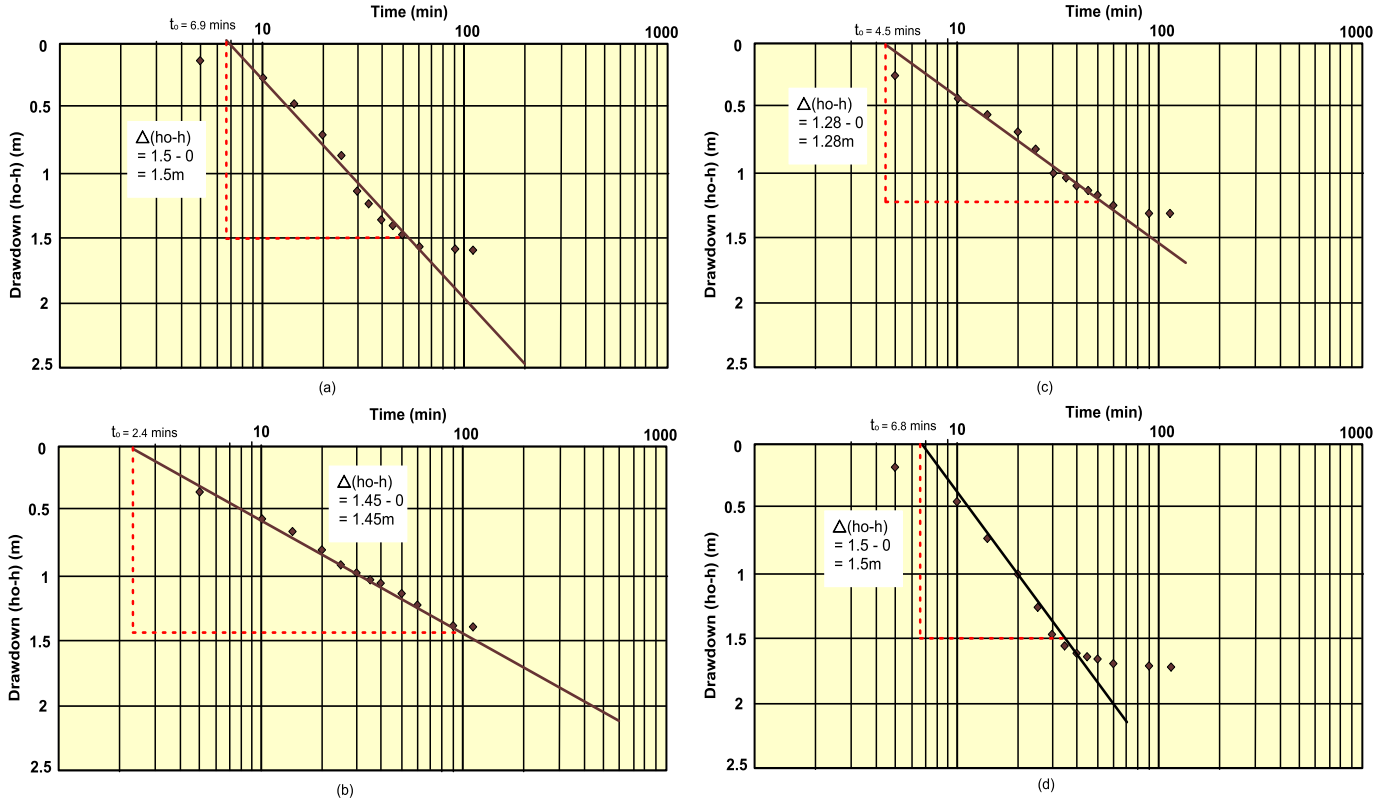

Figure 16: Typical pumping test curves for wells across the three geological units (a) W-23 -gneiss (b) W-35 – granite (c) W-46 - migmatite (d) W-53 – gneiss

The data acquired from fifty eight (58) open wells in Table 4, showed total depth of well investigated ranging from 6.5 (granite; W-4 & 38) – 15.1 m in granite W-12 (avg. 10.1 m). The water column which is storage/reservoir potential of the wells ranged from 2.1 m in W-46 (migmatite) to 9.0 m in W-17 migmatite (avg. 4.5 m) in migmatite rocks. The SWL varied from 2.5 m in migmatite (W-18) to 8.2 m in W-3&12 granite (avg. 5.5 m), with corresponding hydraulic head of 246.1 – 267.8 m above the seal level (avg. 256.0 m). The thickness of the vadose zone which corresponds to the static water level (SWL) is generally moderate i.e. above 5 m, which is capable of providing average daily consumption for domestic needs. The hydraulic conductivity, transmissivity, and storativity was obtained from the pumping test, with typical pumping test data/curves is shown in Figure 15 and Table 5. The K ranged from 0.41 (granite) to 0.55 m/d in migmatite (0.48 m/d avg.), transmissivity 1.16 (W-46; migmatite) – 4.97 m^2/d (W-17; migmatite) with average value of 2.18 m^2/d. The storativity (Sr) varied from 0.0057 in W-02 (gneiss) to 0.0227 in W-01 (granite). The regression model (equation 11) was used to predict the storativity especially in locations where pumping test was not carried. The empirical relationship between transmissivity and storativity, gives high positive linear correlation of 0.7076. Storativity is the product

of the specific storage and the aquifer thickness. Consequently, the average storativity (Sr) or coefficient of storativity is greater than 0.005 which suggests an unconfined aquifer. The results of the well hydraulics correlate well with those estimated for the VES locations which delineated 80 % of the study area to be weathered aquifer.

Storativity = 0.0095 (x) + 0.0437 (11)

Where x is transmissivity

Table 5: Typical field data obtained during the pumping test for some wells

Time (min)	W-23		W-35		W-46		W-53	
	Drawdown (m)	GWL (m)	Drawdown (m)	GWL (m)	Drawdown (m)	GWL (m)	Drawdown (m)	DWL (m)
0	0	5.5	0	6.5	0	5.5	0	4
5	0.21	5.71	0.38	6.88	0.25	5.75	0.2	4.2
10	0.3	5.8	0.59	7.09	0.45	5.95	0.46	4.46
15	0.49	5.99	0.77	7.27	0.59	6.09	0.8	4.8
20	0.7	6.2	0.84	7.34	0.7	6.2	1.07	5.07
25	0.79	6.29	0.9	7.4	0.87	6.37	1.32	5.32
30	1.2	6.7	0.95	7.45	1.01	6.51	1.56	5.56
35	1.31	6.81	1.06	7.56	1.11	6.61	1.63	5.63
40	1.38	6.88	1.14	7.64	1.19	6.69	1.67	5.67
45	1.42	6.92	1.2	7.7	1.26	6.76	1.7	5.7
50	1.53	7.03	1.28	7.78	1.31	6.81	1.71	5.71
60	1.54	7.04	1.33	7.83	1.33	6.83	1.71	5.71
90	1.54	7.04	1.4	7.9	1.35	6.85	1.71	5.71
120	1.54	7.04	1.4	7.9	1.35	6.85	1.71	5.71
T (m^2/min)	0.19		0.19		0.22		0.19	
S	0.0227		0.0057		0.01392		0.01395	

3.3 Hydrogeological Parameters Modeling and Groundwater Potential Mapping

Empirical model (Table 6) was developed for the three geological units (migmatite, granite, and gneiss), by plotting formation factor on x-axis and hydraulic conductivity on y-axis. All the rock units showed positive correlations in descending order as: granite (0.3778), migmatite (0.1057), and gneiss (0.0641). The modeling of the water bearing unit potentiality zones was done using groundwater potential index values (GWPIV) to produce groundwater potential map in Figure 14c and the obtained values for all rated parameters are shown in Table 8. The GWPIV has proved been identified as one of the veritable tools in groundwater assessment and management. Therefore, in this study, multi-criteria decision analysis (MCDA) was done using analytical hierarchy process (AHP) by Saaty (1980). The AHP is a theory of measurement for dealing with quantification and/or intangible criteria that has found rich applications in decision theory, conflict resolution and in models of the brain (Vargas, 1990). The decision applications of the AHP are carried out in two phases: hierarchic design and evaluation using paired comparisons. The normal procedure for AHP was involved in this study by prioritizing the hydrogeologic parameters according to their importance in groundwater accumulation; then the parameters are pair-wise in a matrix form using Saaty (1980) scale of importance, where 1, 3, 5, 7, and 9 are equal, moderate, strong, very strong, and extreme importance respectively; while 2, 4, 6, and 8 are intermediate values; and 1/3, 1/5, 1/7, and 1/9 are values for inverse comparison.

The average values of the relative values in every row are determined, and this gives the criteria weights; consequently the consistency ratio was determined by multiplying the pair-wise comparison matrix with criteria weights calculated for each row, and the average value determined to obtain the weighted sum value. Thereafter, the weighted sum value is divided by criteria weights to obtain consistency ratio for each of the rows. Hence, the average consistency ratio is obtained as Lambda (λ_{max}).

Table 6: Empirical Relationship between hydraulic conductivity and formation factor for different water bearing formations derived geological units

S/Nos.	Geological units	Exponential Equation	Correlation coefficient
1	Migmatite	$y = 0.6373e^{-0.041x}$	0.1057
2	Granite	$y = 0.8816e^{-0.422x}$	0.3778
3	Gneiss	$y = 0.8387e^{-0.2590x}$	0.0641

The next is the determination of consistency index (CI) using equation 12. It is the consistency index of a pairwise comparison matrix which is generated randomly, random index depends on the number of elements which are compared as shown in Table 6.

$$CI = \frac{\gamma_{max} - n}{n-1} \quad (12)$$

Where n is the number of parameters compared.

The criteria weight was tested to know its accuracy, reliability, credibility, and consistency (Saaty, 2008, 1990) in predicting groundwater yield in the study area by dividing the CI with random consistency index value obtained in Table 7 (Saaty, 2006) and the resulted value (0.095 obtained from this study) must be less than 0.10, which is the rule of the process. The obtained weights (w) were used to rate the parameters accordingly (Table 8) as AQT - aquifer layer thickness (0.07), AQR - aquifer layer resistivity (0.10), OVT - overburden thickness (0.16), TR - transverse resistance (0.19), TMY - transmissivity (0.26), CoA - coefficient of anisotropy (0.22). In generating groundwater potential index values (GWPIV), the rating (r) obtained from AHP was multiplied with the weights (which varied from 1 to 5) based on their degree of relevance in groundwater storage and utilization (Table 8), and were summed up (equations 13-14).

$$GW = f(AQT, AQR, OVT, TR, TMY, COA) \quad (13)$$

Therefore the GWPIV was determined using the expression below:

$$\text{GWPIV} = AQT_w AQT_r + AQR_w AQR_r + OVT_w OVT_r + TR_w TR_r + TMY_w TMY_r + COA_w COA_r \quad (14)$$

Thematic layers of the parameters were generated using QGIS software; and the same software was used to do the classification, and produced the GWPIV and subsequent groundwater potential map. The GWPIV was ranked as very low: 0.0 – 1.0; low: 1.0 – 2.0; moderate: 2.0 – 3.0, high: 3.0 – 4.0, and very high greater than 4. Thus the GWPIV ranged from granite 1.53 (VES 14; weathered aquifer) – migmatite 3.50 (VES 47; weathered aquifer) with an average of 2.18 indicating moderate groundwater potential. The developed groundwater potential map (Figure 11c) distinguished the area into two major potential zones, with prominent moderate zone constituting 90 % of the study area. The low potential zone are observed sporadically in the area and constitute 10 % of the study area, with notable places of occurrence included central and northwestern parts. However, the longitudinal unit conductance (LUC) recorded values ranging from 0.0514 – 0.8705 mhos (with regional average of 0.219876

mhos); while migmatite recorded 0.0730 – 0.2669 mhos (0.1641 mhos avg.); granite (0.0514 – 0.8705 mhos; 0.2678 mhos avg.); and gneiss recorded 0.0734 – 0.4288 mhos (0.2111 mhos avg.). Using Table 10, the groundwater system in the study area is weak, although the northwest and central parts appear less weak, as shown in spatial distribution map of LUC in Figure 14b.

Table 7: Random Consistency Index Table for number of parameter (N) and corresponding random value (Saaty, 2006)

N	1	2	3	4	5	6	7	8	9	10
RV	0	0	0.52	0.89	1.11	1.25	1.35	1.40	1.45	1.49

Table 8: Probability rating, normalized weight for different classes of parameters used in deriving the GWPIV

	Parameter	Range	Weight	Remark	Rating
1	Aquifer Layer Thickness (m)	0 – 5	1	Very Low	0.07
		6 – 10 11 – 15 16 - 20	2 3 4	Low Moderate High	
		>20	5	Very High	
2	Aquifer Layer Resistivity (ohm-m)	1 – 100 (Clay)	1	Very Low	0.10
		101 – 250 (Sandy clay)	2	Low	
		251 – 350 (Clayey sand)	3	Moderate	
		351 – 750 (Sand/Fractured aquifer)	5	Very High	
3	Overburden Thickness (m)	1 – 10	1	Low	0.16
		11 – 20	2	Medium	
		21 – 30 >30	3 5	High Very High	
4	Transverse Resistance (ohm-m^2)	1 – 5000	1	Low	0.19
		5001 – 10000	3	Fair	
		>10000	5	High	
5	Transmissivity (m^2/d)	1 – 10	1	Low	0.26
		11 – 20	3	Moderate	
		>20	5	High	
6	Coefficient of Anisotropy	1.1 – 1.15 1.15 – 1.19 1.19 – 1.25 1.25 – 1.30 1.30 – 2.0	1 2 3 4 5	Very Low Low Moderate High VeryHigh	0.22

Table 9: Summary of the obtained values for the seven parameters pair-wise and resulted GWPIV

East	Aquifer	VES No.	AQR	AQT	OVT	TR	T	COA	GWPIV	GWPIV (%)	GWP
Migmatite	WL	1	0.2	0.28	0.32	0.2	0.78	0.44	2.22	44.0	Moderate
Migmatite	WL	2	0.2	0.28	0.32	0.2	0.26	0.44	1.7	33.7	Low
Migmatite	WL	3	0.2	0.35	0.48	0.2	0.26	0.44	1.93	38.2	Low
Granite	WL	4	0.1	0.28	0.32	0.2	0.26	0.44	1.6	31.7	Low
Granite	WL	5	0.2	0.35	0.8	0.6	0.78	0.66	3.39	67.1	High
Granite gneiss	WL	6	0.1	0.28	0.48	0.2	0.26	0.66	1.98	39.2	Low
Granite gneiss	FB	7	0.2	0.21	0.48	1	0.26	0.44	2.59	51.3	Moderate
Granite gneiss	FB	8	0.1	0.28	0.48	0.6	0.26	0.22	1.94	38.4	Low
Migmatite	FB	9	0.1	0.28	0.8	1	0.26	0.66	3.1	61.4	High
Granite gneiss	WL	10	0.1	0.35	0.8	0.2	0.26	0.44	2.15	42.6	Moderate
Migmatite	WL	11	0.2	0.28	0.48	0.2	0.26	0.44	1.86	36.8	Low
Granite	WL	12	0.1	0.28	0.32	0.2	0.26	0.44	1.6	31.7	Low
Granite	WL	13	0.1	0.35	0.48	0.2	0.26	0.44	1.83	36.2	Low
Granite	WL	14	0.1	0.21	0.32	0.2	0.26	0.44	1.53	30.3	Low
Granite	WL	15	0.2	0.35	0.8	0.6	0.26	0.44	2.65	52.5	Moderate
Granite	WL	16	0.2	0.28	0.8	0.6	0.26	0.44	2.58	51.1	Moderate
Granite gneiss	FB	17	0.1	0.21	0.48	0.2	0.26	0.44	1.69	33.5	Low
Granite	WL	18	0.2	0.28	0.48	0.2	0.26	0.44	1.86	36.8	Low

Table 9: Summary of the obtained values for the seven parameters pair-wise and resulted GWPIV

East	Aquifer	VES No.	AQR	AQT	OVT	TR	T	COA	GWPIV	GWPIV (%)	GWP
Granite	WL	19	0.3	0.21	0.32	0.6	0.26	0.44	2.13	42.2	Moderate
Migmatite	WL	20	0.1	0.35	0.48	0.2	0.26	0.44	1.83	36.2	Low
Migmatite	WL	21	0.2	0.28	0.32	0.2	0.26	0.44	1.7	33.7	Low
Granite gneiss	FB	22	0.1	0.28	0.48	0.6	0.78	0.66	2.9	57.4	Moderate
Granite gneiss	FB	23	0.2	0.28	0.8	1	0.26	0.66	3.2	63.4	High
Granite gneiss	FB	24	0.2	0.28	0.48	0.6	0.26	0.44	2.26	44.8	Moderate
Granite	WL	25	0.1	0.35	0.48	0.2	0.26	0.44	1.83	36.2	Low
Granite	WL	26	0.1	0.28	0.32	0.2	0.26	0.44	1.6	31.7	Low
Migmatite	WL	27	0.1	0.28	0.48	0.2	0.26	0.44	1.76	34.9	Low
Migmatite	WL	28	0.2	0.28	0.48	0.6	0.26	0.44	2.26	44.8	Moderate
Granite	FB	29	0.2	0.28	0.48	0.6	0.26	0.66	2.48	49.1	Moderate
Granite	WL	30	0.1	0.28	0.48	0.2	0.26	0.44	1.76	34.9	Low
Granite	WL	31	0.1	0.28	0.48	0.2	0.26	0.44	1.76	34.9	Low
Migmatite	FB	32	0.2	0.28	0.8	0.6	0.26	0.44	2.58	51.1	Moderate
Granite gneiss	WL	33	0.1	0.28	0.32	0.2	0.26	0.44	1.6	31.7	Low
Migmatite	WL	34	0.1	0.35	0.48	0.2	0.26	0.44	1.83	36.2	Low
Migmatite	WL	35	0.2	0.35	0.48	0.2	0.26	0.44	1.93	38.2	Low
Migmatite	WL	36	0.2	0.28	0.48	0.6	0.26	0.44	2.26	44.8	Moderate
Granite	WL	37	0.1	0.35	0.48	0.2	0.26	0.44	1.83	36.2	Low
Granite	WL	38	0.1	0.28	0.48	0.2	0.26	0.44	1.76	34.9	Low
Granite	WL	39	0.2	0.28	0.32	0.2	0.26	0.44	1.7	33.7	Low
Granite	WL	40	0.2	0.21	0.32	0.2	0.26	0.44	1.63	32.3	Low
Granite gneiss	WL	41	0.2	0.14	0.32	0.2	0.26	0.44	1.56	30.9	Low
Granite gneiss	WL	42	0.5	0.28	0.48	1	0.26	0.44	2.96	58.6	Moderate
Granite gneiss	FB	43	0.1	0.21	0.8	1	0.26	0.88	3.25	64.4	High
Granite gneiss	WL	44	0.1	0.28	0.48	0.6	0.26	0.44	2.16	42.8	Moderate
Migmatite	WL	45	0.5	0.21	0.48	0.6	0.26	0.66	2.71	53.7	Moderate
Granite	WL	46	0.1	0.35	0.8	0.2	0.78	0.44	2.67	52.9	Moderate
Migmatite	WL	47	0.5	0.28	0.8	1	0.26	0.66	3.5	69.3	High
Migmatite	WL	48	0.5	0.28	0.48	0.6	0.26	0.66	2.78	55.0	Moderate
Granite	WL	49	0.5	0.21	0.32	1	0.26	0.44	2.73	54.1	Moderate
Granite	WL	50	0.1	0.35	0.48	0.2	0.26	0.44	1.83	36.2	Low

Table 10: Longitudinal unit conductance and corresponding protective rating (Falowo, 2022)

Total Longitudinal unit Conductance (mhos)	Rating of overburden's aquifer protective capacity
<0.10	Poor
0.1 – 0.49	Weak
0.5 – 0.99	Moderate
1.0 - 4.99	Good
5.0 – 10.0	Very good
>10.0	Excellent

4. Conclusion

Hydrogeologic studies has been carried out in Ile Oluji, Ondo State, Southwestern Nigeria using multi-criteria decision analysis using geographic information system supported analytical hierarchy process on six hydrogeologic/geoelectric parameters comprising aquifer layer thickness, aquifer layer resistivity, overburden thickness, transverse resistance, transmissivity, and coefficient of anisotropy. These parameters were used to estimate the GWPIV, which was lower in granite, and higher in migmatite. The average value of GWPIV suggested moderate groundwater potential constituting 90 % of the study area. The low potential zone (10 % of the study area) are observed sporadically in the central and northwestern parts. The longitudinal unit conductance recorded weak regional average of 0.219876 mhos, suggestive of high groundwater system vulnerability to pollution in the study area, and relatively less-weaker in granite, while the northwest and central parts appear less weak. Nonetheless, the water table aquifer (accounts for 80%) and the fracture basement (constitutes 20%, frequently occurring in gneissic environment). The average overburden thickness is high in gneiss and lesser in migmatite, and granite terrain.

Acknowledgements

The author is grateful to TETFund, Nigeria (under the Institution Based Research) Nigeria. Special appreciation to all students of especially Higher National Diploma students of Civil Engineering Technology Department, for the assistance rendered during data acquisition.

References

Adagunodo, M.K., Sunmonu, L.A., Aizebeokhai, A.P., Oyeyemi, K.D., Abodunrin, F.O., 2018. Groundwater Exploration in Aaba Residential Area of Akure, Nigeria. Front. Earth Science, 66(6), Pp. 1–12, DOI:10.3389/feart.2018.00066.

Adebawore, A.A., Akinyeye, R. O., Awokunmi, E. E., Ayodele, O., Olanipekun, E. O., et al., 2017. Seasonal variations of Heavy Metals in Water Samples from Selected Hand-Dug Wells Close to Petrol Stations in Ile-Oluji, Ondo State, Nigeria. J. of Physical and Chemical

Sciences.V5I3. DOI: 10.15297/JPCS.V5I3.05

Adeleke, O.O., Makinde, V., Eruola, A.O., Dada, O.F., Ojo, A.O., Aluko, T.J. 2015. Estimation of Groundwater Recharges in Odeda Local Government Area, Ogun State, Nigeria using Empirical Formulae. Challenges, 6, Pp. 271–281.

Aina, J.O., Adeleke O.O., Makinde V., Egunjobi, H.A., Biere, P.E. 2019. Assessment of Hydrogeological Potential and Aquifer Protective Capacity of Odeda, Southwestern Nigeria. RMZ – M and G, Vol. 66, Pp. 199–210

Akanbi, O.A. 2016. Use of vertical electrical geophysical method for spatial characterisation of groundwater potential of crystalline crust of Igboora area, southwestern Nigeria. International Journal of Scientific and Research Publications, 6(3), Pp. 399–406.

Akanbi, O.A. 2017. Hydrogeological Characterisation of Crystalline Basement Aquifers of part of Ibarapa Area, Southwestern Nigeria. Ph. D. Thesis. Ibadan-Nigeria: University of Ibadan 2017; Pp. 312.

Akinrinade, O. J., Olabode, O.P. 2015. Integrated geophysical approach to aquifer delineation in crystalline basement environment. International Journal of Scientific and Engineering Research (IJSER), France, 6(10), Pp. 107–127.

Akinrinade, O.J., Adesina, R.B. 2016. Hydrogeophysical investigation of groundwater potential and aquifer vulnerability prediction in basement complex terrain – A case study from Akure, Southwestern Nigeria. RMZ – M&G, Vol. 63 | Pp. 55–066. DOI: 10.1515/rmzmag-2016-0005

Alley, W.M., Leake, S.A., 2004. The journey from safe yield to sustainability. Groundwater, 42(1): 12-16. https://doi.org/10.1111/j.1745-6584.2004.tb02446.x

Assaad, F., LaMoreaux, P.E., Hughes, T. 2004. Field Methods for Geologists and Hydrogeologists. Springer, Berlin.

Bayewu, O.O., Oloruntola, M.O., Mosuroa, G.O., Laniyana, T.A., Ariyo, S.O., Fatoba, J.O. 2018. Assessment of groundwater prospect and aquifer protective capacity using resistivity method in Olabisi Onabanjo University campus, Ago-Iwoye, Southwestern Nigeria. NRIAG Journal of Astronomy and Geophysics, 7, pp. 347–360.

Bell, F.G. 2007. Engineering Geology, Second Edition. Elsevier, 581pp.

Brassington, R. 1988. Field Hydrogeology. Wiley, Chichester, 926pp.

Chaanda, M.S., Alaminiokuma, G.I. 2020. Hydrogeophysical Investigation for Groundwater Resource Potential in Masagamu, Magama area, Fractured Basement Complex, North-Central Nigeria. Malaysian Journal of Geosciences, 4(2): 43-47. DOI:10.26480/mjg.02.2020.43.47

Cosgrove, W.J., Loucks, D.P. 2015. Water Management: Current and Future Challenges and Research Directions. Water Resources Research, 51(6), pp. 4823–4839.

Falowo, O.O. 2022. Modeling of hydrogeological parameters and aquifer vulnerability assessment for groundwater resource potentiality prediction at Ita Ogbolu, Southwestern Nigeria. Modeling Earth Systems and Environment, 21 pp. https://doi.org/10.1007/s40808-022-01490-8

Falowo, O.O., Akindureni, Y., Ojo O. 2017. Groundwater Assessment and Its Intrinsic Vulnerability Studies Using Aquifer Vulnerability Index and GOD Methods. International Journal of Energy and Environmental Science, Vol. 2, No. 5, 2017, pp. 103-116. doi: 10.11648/j.ijees.20170205.13

Falowo, O.O., Daramola, A.S. 2023. Geo-Appraisal of groundwater resource for sustainable exploitation and management in Ibulesoro, Southwestern Nigeria. Turkish Journal of Engineering 2023, 7(3), 236-258, DOI: 10.31127/tuje.1107329

Falowo, O.O., Ojo, O.O., Daramola, A.S. 2020. Groundwater Resource Assessment by Hydraulic Properties Determination for Sustainable Planning and Development in Central Part of Ondo State, Nigeria. Environmental and Earth Sciences Research Journal Vol. 7, No. 1, March, 2020, pp. 1-8 https://doi.org/10.18280/eesrj.070101

FAO/DSMW, 2020. Digital Soil Map of the World at 1,500,000 Scale (Geonetwork). Food and Agricultural Organization https://www.fao.org/soils-portal/data-hub/soil-maps-and-databases/faounesco-soil-map-of-the-world/en/ Accessed 19th January, 2023.

Fetter, C.W. 2007. Applied hydrogeology. 2nd edition. USA: Merrill Publishing Company.

Freeze, R.A., Cherry, J.A. 1979. Groundwater. Prentice-Hall, Englewood Cliffs, New Jersey

Gao, Q., Shang, Y., Hassan, M., Jin, W., Yang, P. 2018. Evaluation of a Weathered Rock Aquifer using ERT Method in South Guangdong, China. Water. 10:1-22. https://doi.org/10.3390/w10030293

Gogoi, U., 2013. Determination of aquifer parameters of the shallow aquifers of Barak valley, Assam, India. Int. Bulletin Water Resources Dev., 1: 1-13.

Halford, K.J., Wright, W.D., Schreiber, R.P., 2006. Interpretation of Transmissivity estimates from single well pumping aquifer tests. Ground Water, 44: 467- 471. DOI: 10.1111/j.1745-6584.2005.00151.x

Harb, N., Haddad, K., Farkh, S., 2010. Calculation of transverse resistance to correct aquifer resistivity of groundwater saturated zones: implications for estimating its hydrogeological properties, Lebanese Science Journal, 11(1), Pp. 105–115.

Harvill, Bell, F.G., 1986. Groundwater Resource Development, Butterworks, London.

Iloeje, N.P. 1981. A New Geography of Nigeria. Longman Publisher Nigeria, pp. 201.

Johnson, T. 2005. A measure of well performance, well problems and aquifer Transmissivity. WRD Technical Bulletin, 2: Pp. 1-2.

Karanth, K.R. 1987. Groundwater Assessment, Development and Management, Tata McGraw Hill Pub. Co. Ltd., New Delhi.

Kruseman, G.P., de Ridder, N.A., 1991. Analysis and Evaluation of Pumping Test Data. International Institute for Land Reclamation and Improvement/ILRI. Wageningen, The Netherlands.

Lewis, M A., 1989. Water: In Earth Science Mapping For Planning, Development AndConservation. Mccall, J and Marker, B; Graham and Trotman (Editors).

Living Atlas, 2020. A-10 m Resolution map of earth's; and surface from 2020, developed by Impact Observatory. https://livingatlas.arcgis.com/landcover/ Accessed on 19th January 2023.

Mandel, S., Shiftan, Z.L., 1981. Groundwater Resources – Investigation and Development, Academic Press, Inc., New York

Mohamaden, M.I., 2016. Delineating groundwater aquifer and subsurface structures by using geoelectrical data: case study (Dakhla Oasis, Egypt). NRIAG J Astron Geophys 5(1): Pp. 247–253. https ://doi.org/10.1016/j.nrjag .2016.05.001

Nigeria Geological Survey Agency (NGSA), 2006. Published by the Authority of the Federal Republic of Nigeria.

Nwosu, L.I., Ekine, A.S., Nwankwo, C.N., 2013. Evaluation of Groundwater Potential from Pumping Test Analysis and Vertical Electrical Sounding Results: Case Study of Okigwe District of Imo State Nigeria. The Pacific Journal of Science and Technology, Volume 14. Number 1,Pp. 536 – 548. http://www.akamaiuniversity.us/PJST.htm

Obaje, N.G., 2009. Geology and Mineral Resources of Nigeria. Springer-Verlag, Berlin, 218p.

Olatunji, S., Issa, U., Ajadi, J., 2022. Groundwater Potential Evaluation in Parts of Southwestern Nigeria Using Dar-Zarouk Parameters. LAUTECH Journal of Civil and Environmental Studies Volume 8, Issue 1; March, 2022, Pp. 8. DOI: 10.36108/laujoces/2202.80.0150

Omer, A.M., 2018. Sustainability Criteria for Water Resource Systems: Sustainable Development and Management. Int. J. Adv. Res. Water Resc. Hydr. Engi., 1(1&2):Pp. 1-19.

Oyegoke, S.O., Adebanjo, A.S., Fayomi, O.O., Obot, O., 2020. Groundwater Prospecting using combined Vertical Electrical Sounding and Borehole Performance. LAUTECH Journal of Civil and Environmental Studies Volume 4, Issue 1; March 2020.

Robinson, E.S., Coruh, C., 1988. Basic Exploration Geophysics, John Wiley and Sons, New York.

Saaty, I.T., 1980. The analytical hierarchy process, New York, McGraw-Hill International.

Saaty, I.T., 1990. How to make a decision: the analytic hierarchy process,

Saaty, I.T., 2006. Rank from comparisons and from ratings in the analytical/network processes. European Journal of Operational Research, Vol. 168, Pp. 557-570.

Saaty, T.L., 2008. There is no Mathematical validity for using Fuzzy Number Crunching in the Analytic Hierarchy Process, Unpublished report.

Sajeena, S., Abdul Hakkim, V.M., Kurien, E.K., 2014. Identification of Groundwater Prospective Zones using Geoelectrical and Electromagnetic Surveys. International Journal of Engineering Inventions, 3(6), Pp. 17–21.

Sameer, S.M., Mustafa, A.S., Al-Somaydaii, J.A., 2021. Study of the Sustainable Water Resources Management at the Upper Euphrates Basin, Iraq. International Journal of Design and Nature and Ecodynamics Vol. 16, No. 2, April, 2021, Pp. 203-210. https://doi.org/10.18280/ijdne.160210

Tartiyus, E.H., Mohammed, I.D., Amade, P., 2015. Impact of Population Growth on Economic Growth in Nigeria (1980–2010). Journal of Humanities and Social Science (IOSR-JHSS), 20(4), Pp. 115–123. DOI: 10.9790/0837-2045115123.

Telford, W.M., Gedart, L.P., Sheriff, R.E., 1990. Applied Geophysics. Cambridge University Press: London, UK. 726.

Ting, C.S., 1993. Groundwater resources evaluation and management studies for the Pingtung Plain, Taiwan. National Science Council, National Pingtung Polytechnic Institute and Faculty of Earth Sciences, Free University, Amsterdam, Pp. 87.

Vargas, L.G. 1990. An overview of the analytical hierarchy process and its applications. European Journal of Operational Research, 48: Pp. 2-8.

Yang, Ch.Ch., Chen, B.Sh., 2004. Key quality performance evaluation using Fuzzy AHP, Journal of the Chinese Institute of Industrial Engineers, Vol. 21, No. 6, Pp. 543-550.